Approved for public release; distribution is unlimited.

Spectral Analysis of Vortex/Free-Surface Interaction

by

Glenn D. Hofert
Lieutenant, United States Navy
Professional Engineer
M.B.A., National University, 1991
B.N.E., Georgia Institute of Technology, 1986

Submitted in partial fulfillment of the
requirements for the degree of

MASTER OF SCIENCE IN MECHANICAL ENGINEERING

from the

NAVAL POSTGRADUATE SCHOOL

June 1994

Unclassified

SECURITY CLASSIFICATION OF THIS PAGE

REPORT DOCUMENTATION PAGE

Form Approved OMB No. 0704-0188

1a. REPORT SECURITY CLASSIFICATION Unclassified	1b. RESTRICTIVE MARKINGS
2a. SECURITY CLASSIFICATION AUTHORITY	3. DISTRIBUTION AVAILABILITY OF REPORT Approved for public release; distribution unlimited
2b. DECLASSIFICATION/DOWNGRADING SCHEDULE	
4. PERFORMING ORGANIZATION REPORT NUMBER(S)	5. MONITORING ORGANIZATION REPORT NUMBER(S)
6a. NAME OF PERFORMING ORGANIZATION Naval Postgraduate School; 6b OFFICE SYMBOL (If applicable) ME	7a. NAME OF MONITORING ORGANIZATION Naval Postgraduate School
6c. Address (City, State, and ZIP Code) Monterey, CA 93943-5000	7b. ADDRESS (City, State, and ZIP Code) Monterey, CA 93943-5000
8a. NAME OF FUNDING/SPONSORING ORGANIZATION; 8b OFFICE SYMBOL (If applicable)	9. PROCUREMENT INSTRUMENT IDENTIFICATION NUMBER
8c. ADDRESS (City, State, and ZIP Code)	10. SOURCE OF FUNDING NUMBERS: PROGRAM ELEMENT NO. / PROJECT NO. / TASK NO. / WORK UNIT ACCESSION NO.

11. TITLE (Include Security Classification) Spectral Analysis of Vortex/Free-Surface Interaction

12. PERSONAL AUTHOR(S) GLENN D. HOFERT

13a. TYPE OF REPORT	13b. TIME COVERED	14. DATE OF REPORT (Year, Month, Day)	15. PAGE COUNT
Thesis for Master of Science in Mechanical Engineering	From:	June 1994	74

16. SUPPLEMENTARY NOTATION The views expressed in this thesis are those of the author and do not reflect the official policy or position of the Departm of Defense or the U. S. Government.

17. COSATI CODES			18. SUBJECT TERMS (Continue on reverse if necessary and identify by block number)
FIELD	GROUP	SUB-GROUP	Surface Disturbances, Scars, Striations, Trailing Vortices, Vortex Dynamics

19. ABSTRACT (Continue on reverse if necessary and identify by block number)

The unsteady flow phenomena resulting from the interaction of vorticity with a free surface has been investigated through the use of a three-color Laser-Doppler-Velocimeter. The vorticity field was provided by a single tip vortex generated by an airfoil, placed in the test section of a recirculating water tunnel at a suitable angle of attack. All of the statistical quantities of flow such as turbulence and Reynolds stresses and in particular the spectrum of the fluctuations have been measured and analyzed. The results have shown that the free surface redistributes part or all of the normal turbulent kinetic energy into streamwise and spanwise components. Furthermore, the energy spectra have also shown that there exists an energy gradient on the free surface, on either side of the vertical passing through the original vortex. It is believed that the scars observed on the free surface are a consequence of the matching of the Bragg wave length with the wave length of the surface signatures within a particular spectrum.

20. DISTRIBUTION/AVAILABILITY OF ABSTRACT	21. ABSTRACT SECURITY CLASSIFICATION	
☒ UNCLASSIFIED/UNLIMITED ☐ SAME AS RPT. ☐ DTIC USERS	Unclassified	
22a. NAME OF RESPONSIBLE INDIVIDUAL	22b TELEPHONE (Include Area code)	22c. OFFICE SYMBO
Professor T. Sarpkaya	(408) 656-3425	ME-SL

DD Form 1473, JUN 86 Previous editions are obsolete. SECURITY CLASSIFICATION OF THIS PAGE

Unclassified

ABSTRACT

The unsteady flow phenomena resulting from the interaction of vorticity with a free surface has been investigated through the use of a three-color Laser-Doppler-Velocimeter. The vorticity field was provided by a single tip vortex generated by an airfoil, placed in the test section of a recirculating water tunnel at a suitable angle of attack. All of the statistical quantities of flow such as turbulence and Reynolds stresses and in particular the spectrum of the fluctuations have been measured and analyzed. The results have shown that the free surface redistributes part or all of the normal turbulent kinetic energy into streamwise and spanwise components. Furthermore, the energy spectra have also shown that there exists an energy gradient on the free surface, on either side of the vertical passing through the original vortex. It is believed that the scars observed on the free surface are a consequence of the matching of the Bragg wave length with the wave length of the surface signatures within a particular spectrum.

TABLE OF CONTENTS

LIST OF FIGURES

LIST OF SYMBOLS

c	= Chord length of foil
Eu	= Energy spectrum for u'
Ev	= Energy spectrum for v'
Ew	= Energy spectrum for w'
ho	= Depth of vortex from free surface
k	= $\Gamma/2\pi$
Rc	= Vortex core radius
Re	= Reynolds number, $U_o c/\nu$
U_o	= Velocity of ambient flow
u	= Axial component of velocity
u'	= rms value of u', normalized by U_o
v	= Transverse component of velocity
v'	= rms value of v', normalized by U_o
w	= Vertical component of velocity
w'	= rms value of w', normalized by U_o
x	= Axial coordinate, origin at free surface
y	= Lateral coordinate, origin at free surface
y'	= Lateral coordinate, origin at the vortex
Z	= Complex variable, y' + iz'
z	= Vertical coordinate, origin at free surface
z'	= Vertical coordinate, origin at vortex
Γ	= Circulation of vortex
ν	= Kinematic viscosity

ACKNOWLEDGMENTS

I would like to take this opportunity to thank Mr. Mike Kotas and all of the employees of Dantec Measurement Technology who were ever so instrumental in the configuration and installation of the LDV system that made all of the measurements in this thesis possible. The seeding particles were kindly provided by Mr. Leroy Frank of the Mearl Corporation.

Thanks are also due for the spirited assistance in the laboratory that was unselfishly and freely offered by Mr. Fisher Yue.

To my wife, I can not offer enough gratitude for your patience and loving support throughout this whole ordeal.

Lastly, and certainly most importantly, my heartfelt appreciation goes out to Distinguished Professor Sarpkaya whose patience, guidance and instruction were more than a person could ever ask for or expect. From you I have earned more than an education. I have learned the essence of what it takes to be a professional both in my career aspirations and what life has to offer beyond. Your personal integrity and undying devotion to the field of fluid mechanics has set a precedence for this educational institution. It seems I shall never be able to fully repay you for these past few years.

I. INTRODUCTION

Mass, momentum, vorticity, and heat fluxes across a sharp-density interface and, most notably, across the air-sea interface, depend on macro- and microscale interactions between the adjacent layers. The interest in these highly nonlinear, coupled, and mostly turbulent processes spans over many subjects such as physical oceanography, meteorology, acoustics, signatures of subsurface coherent structures, and internal waves. The prevailing body of evidence shows that (Brandt *et al.*, 1992) these fluxes involve the interaction of many degrees of freedom over a broad range of spatial and temporal scales, ranging from those on which energy is dissipated to scales associated with the depth of the mixed layers. Also, there is growing evidence that there is a slow local reverse energy cascade (through merging of the same-sign wall-normal vorticity), and that the topological features of the two-dimensional turbulence on the free surface are inherent products of the mutual interaction of the free surface with the three-dimensional turbulence beneath the free surface fueling the entire process.

Earlier works were motivated by the need to understand the physics of gas transport and hence the relationship between molecular and turbulent diffusion and gas transfer (Dickey *et al.*, 1984). In fact, some of the fundamental research on the interaction of turbulence with the free surface was carried out in connection with the gas-transport phenomenon. The more recent interest comes from free-surface hydrodynamics and free-surface signatures of subsurface coherent structures. The discovery of the Synthetic Aperture Radar (SAR) images of ship wakes (a dark and narrow V-shaped region, bounded by two non-parallel bright lines) gave fresh impetus to the

numerical and experimental investigations of the near-surface flows resulting from the motion of floating or submerged bodies, submerged jets, trailing vortices, and vortex rings.

When a trailing vortex couple, generated by a lifting foil, rises toward the free surface, with or without mutual induction instability and/or vortex breakdown, the vortices and/or the crude vortex rings give rise to surface disturbances (whirls, scars, and striations). These were first reported by Sarpkaya and Henderson (1984, 1985) and Sarpkaya (1985, 1986). The striations are essentially three-dimensional free-surface disturbances (which appear as ridges) normal to the direction of the motion of the lifting surface, and come into existence when the vortex couple is at a distance equal to about one initial vortex separation from the free surface. The scars are small free-surface depressions, comprised of many randomly distributed whirls, and come into existence towards the end of the pure striation phase, when the vortices are at a distance equal to about sixty percent of the initial vortex separation from the free surface. When the vortices migrate large distances upward, the vortex couple usually undergoes both short–wavelength and long–wavelength sinusoidal instability and often breaks up into isolated rings (Sarpkaya and Suthon, 1991).

Even though it was fully realized at the outset that the problem ultimately to be solved is the understanding of the three-dimensional nature of the phenomenon, the relative ease of the two dimensional counterpart has attracted the immediate attention of experimentalists and numerical analysists alike (see, e.g., Sarpkaya *et al.* 1988; Willmarth *et al.* 1989; Marcus and Berger 1989; Telste 1989; Ohring and Lugt 1989; and Dommermuth 1992,

1993). Most of the numerical simulations dealt with the inviscid, two-dimensional interaction between a couple of heterostrophic (opposite sign) line vortices and a free, initially planar, surface. In these calculations, the critical time at which the numerical instability manifests itself does not correspond to the instability of the free surface or to its maximum position. The calculations of Ohring and Lugt are for a two-dimensional laminar flow at relatively small Reynolds numbers. Observations and measurements strongly suggest that the three-dimensional nature of the surface deformation, the surface renewal by large turbulent eddies, the quasi-two-dimensionalization of the near-surface turbulence, and the *reverse energy cascade* are essential to the existence of the scars and striations and to the evolution of long-lived organized structures amidst a rapidly decaying turbulent medium. It should be noted that structures which grow by merging of like-sign surface-normal vorticity continuously replenish those which have been created at earlier times.

It is evident from the foregoing that the vorticity/free-surface interaction or mutual modification requires a deeper understanding of the physics of the various phenomena, particularly when the vorticity is in a turbulent state. This is not a clean problem, physically, experimentally, or numerically. Bubbles and surfactants change the surface tension gradients, affect the damping of centimeter and decimeter range waves, and the generation of new vorticity. The change in the mean velocity distorts the vorticity of the turbulence and, thus, the problem is considerably more difficult than the 'moving-wall' problem of Uzkan and Reynolds (1967) where there is no change in the mean velocity (zero mean shear) and the boundary is rigid (see

also, Thomas and Hancock, 1977; Hunt and Graham, 1978; and Biringen and Reynolds, 1981). The deformation of the free surface makes the measurements difficult even for laminar states. The turbulence is not nominally homogeneous or isotropic either in the horizontal planes or in the bulk in any vertical plane. Often, an intentionally imbedded semi-coherent source (e.g., a vortex) is not too far from the free surface and the turbulence characteristics (particularly their gradients in the lateral direction in the region of interest) are strongly affected by the details of the generation mechanism. The spontaneous reformation of coherent structures (near the free surface) out of the randomized field or the semi-coherent submerged source depends on the type of flow giving rise to vorticity (bottom-wall boundary layer as in an open channel, an oscillating submerged grid, a submerged jet, a pair of ascending trailing vortices, vortex rings, turbulent ship wakes). In comparison, the characteristics of grid-stirred tank and open-channel turbulence are somewhat simpler.

The numerical calculations are just as hampered by the nonlinear free surface conditions, turbulent nature of the interaction, and the increasing degree of realism required by the investigation. In spite of these obstacles, the mutual interaction of vorticity with a deformable fluid interface; generation of surface tension gradients, tangential stresses, and secondary vorticity due to surface deformations and contamination; generation of gravity and capillary waves; the flattening of eddies and the preferential attenuation of low frequencies (large scales) near the free surface; the sharp reduction in the vertical velocity fluctuations accompanied by an amplification of horizontal turbulent velocities; the extent of the anisotropic turbulence field; the

remarkable phenomenon of vortex-tube splitting and the connection of the tube ends with the free surface as swirling eddies or whirls; the preferential merging of whirls, the reverse energy cascade; and the understanding of the physics of coherent structures and turbulent mixing near density interfaces have attracted considerable attention in connection with the occurrence and longevity of surface signatures and SAR images (Brumley, 1984; Brumley and Jirka, 1987; Dickey *et al.*, 1984; Komori, *et al.*, 1982; Sarpkaya, 1986; Loewen *et al.* 1986; Sarpkaya *et al.*, 1988; Sarpkaya, 1991; Sarpkaya, 1992a; Brumley and Jirka, 1987; Rashidi and Banerjee, 1988; Anthony and Willmarth, 1992; Lam and Banerjee, 1992; Komori *et al.*, 1993; and Sarpkaya and Neubert 1993).

Extensive reviews of the interaction of a pair of heterostrophic vortices with a free surface are given by Sarpkaya (1986, 1992a, 1992b) and by Sarpkaya *et al.* (1993, 1991, 1994). The quasi two- dimensionalization of turbulence in various types of flows (Jacquin *et al.*, 1989 and Hunt and Graham, 1978), in general, and near a free surface (Loewen *et al.* 1986; Brumley, 1984; Dickey *et al.*, 1984; Komori, *et al.*, 1982; Rashidi and Banerjee, 1988; Sarpkaya and Suthon, 1991; Lam and Banerjee, 1992; Komori *et al.*, 1993; and Anthony and Willmarth, 1992), in particular, and the evolution of coherent structures at deformable fluid interfaces have emerged as fundamental phenomena during the past decade. Their understanding is complemented by the existing knowledge base spanning a period of nearly forty years on turbulent diffusion across density discontinuities (Rouse and Dodu, 1955; Hannoun *et al.* 1978; and Hannoun and List, 1978) and on coherent structures in canonical as well as non-equilibrium turbulent flows (Robinson, 1991; Smith *et al.* 1991; Sarpkaya, 1993). The deformability of the fluid interface and the type of

coherent turbulence source beneath the free surface add new complexities to the near-surface phenomena.

One of the simplest possible flows relevant to the dynamical processes in vorticity/free-surface interaction which can be studied in relative isolation, without the complications and competing influences that normally occur in a fully turbulent ship wake, is the interaction of a single turbulent vortex with the free surface. The modulations of the flow field and the topological features of turbulence near the free surface are not expected to be similar either to those induced by a streamwise vortex in or near a rigid-wall boundary layer (Harvey and Perry, 1971; Shabaka *et al.* 1985) or to those resulting from the mutual interaction of the free surface with a three-dimensional turbulence beneath the free surface. There is growing evidence from open channel and oscillating-grid experiments that **any turbulence field** approaching the free surface may be restructured and two-dimensionalized by the free surface and forced to cascade some of its energy in the reverse direction through the occasional merging of the resulting surface-normal, like-sign, vortical structures. A streamwise vortex below the free surface, however, enhances the above processes through the ejection of vorticity in quasi-coherent quanta from the edges of its core (Sarpkaya, 1992) and gives rise to lateral gradients in micro- and macro-scales of turbulence. The emergence of fairly organized scale bands on either side of the vortex, rather than randomly distributed vortical structures, should lead to further merging among like-sign and equi-strength vortices and enhance the longevity of the surface signatures. Such an arrangement of organized bands of vortical structures or whirls, emerging from the occasional merging of vortex

filaments, at or near the free surface is not expected from an arbitrary three-dimensional turbulence field interacting with the free surface.

The investigation described herein is a continuation of the work carried out at the Naval Postgraduate School and deals specifically with the turbulence characteristics, including spectra, of the surface layer where the most intense and interesting vortex/free-surface interaction takes place.

II. NUMERICAL ANALYSIS

A key to the quantification of the flow field created by the interaction of the mean flow, streamwise vortex, and the free surface was to establish a model for a deeply-submerged vortex in terms of its core size Rc, strength Γ, and maximum velocity $V_o = \Gamma/2\pi Rc$. The Rankine and Lamb vortices were rejected as being unrepresentative of a trailing vortex. Instead, a Rosenhead (1930) vortex was chosen. Then the transverse and vertical components of velocity (v and w) along a horizontal line $Z = y' + iz'$ where y' and z' are measured from the vortex (see Figure 1) are given by,

$$\frac{v}{V_o} = 1.548 \frac{(z / Rc)}{(y / Rc)^2 + (z / Rc)^2 + 1}$$

$$+ \frac{2(ho / Rc) - z / Rc}{(y / Rc)^2 + [2(ho / Rc) - z / Rc]^2 + 1} \qquad 1(a)$$

and

$$\frac{w}{V_o} = \frac{2(y / Rc)}{(y / Rc)^2 + (z / Rc)^2 + 1}$$

$$- \frac{2(y / Rc)}{(y / Rc)^2 + [2(ho / Rc) - z / Rc]^2 + 1} \qquad 1(b)$$

Strictly speaking, neither the shape of the vortex core nor the vortex strength can be precisely simulated with a relatively simple model because of the effect of the image flow (mutual straining of the vortex cores) and the free surface deformation. Nevertheless, the measurements may be made to

match those predicted from Eqs. (1a) and (1b) in terms of two experimentally determined values: core radius Rc and the circulation Γ, for a deeply-submerged vortex which is not to be materially affected by the surface disturbances.

III. EXPERIMENTAL EQUIPMENT

The experiments were conducted in a low turbulence water tunnel with an open test section 38.3 cm wide, 36.3 cm deep (maximum), and 127 cm long. The turbulence management system is located upstream of the test section. It consists of a honeycomb and a fine-mesh screen. The tunnel is driven by a 50 Hp centrifugal pump. A second but smaller pump continuously circulated the tunnel water through a micro filtration system to remove rust and other suspended fine particles, down to about 1 mm, from the water (the filtration system was turned off during the experiments). A skimmer, placed upstream of the turbulence management system and connected to another filter, was operated continuously to maintain the free surface clean.

A 6% thick, rectangular planform, symmetric, Joukowski half-span foil with an effective aspect ratio of 10.4 was used to generate a 'single' trailing vortex. The tip of the foil was carefully rounded. The model foil was mounted in a rotatable cylindrical base, embedded into the bottom of the test-section floor. The angle of attack was set at 10^{o} and the water level was held constant. The interior of the model was hollowed and connected to a dye reservoir to seed the vortex core with a fluorescent dye. The leading edge of the foil was 3.7 chord lengths downstream of the test section entrance. The lateral position of the foil was offset by about two vortex-core radii Rc that the vortex entered the working section fairly near the mid-plane where the measurements are made. The reason for the offset is that there is necessarily a wake side-wash (a flux of lateral momentum) due to the lift or the transverse force of magnitude $\rho U_o \Gamma b_o$ acting on the foil, where b_o is the semi-span.

The mean velocities and turbulence intensities were measured with a three-color Dantec Laser-Doppler Velocimeter system. Bragg-cell frequency shifting by 40 MHz was used in all channels to detect the flow reversals. The probe volume (approximately 100 mm in diameter) was positioned at the required location by use of a remotely driven x-y-z traversing unit. The scattering particles used were titanium dioxide of rutile crystalline form and were approximately 10 microns in size. All measurements were made using 1024 point ensembles. The data are reported without any velocity-bias-correction.

Uncertainty for the dimensionless mean velocities is estimated as ±1.5 percent in the core region and as ±0.75 percent outside the core. The rms values u', v', and w' are accurate within ±3 percent. The turbulence intensity in the main flow was about 1 percent. Finally, the uncertainties for the energy spectra are estimated as ±2 percent in the ordinate and ±5 percent in the abscissa.

The initial measurements were dedicated to the establishment of the flow characteristics at the test section. These measurements have shown that the velocity was uniform (except in the boundary layers, of course) within 1%, in both the vertical and horizontal directions.

Two vortex positions relative to the free surface and one measurement station relative to the trailing edge of the foil were considered. For the first case, the vortex axis was placed at ho/Rc = 5.58 from the free surface. Here ho is the depth of the vortex axis and Rc is the core radius. For the second case, the vortex axis was placed at ho/Rc = 1.15. In both cases, the velocity and

turbulence measurements were made along several y/Rc = constant (vertical lines) and z = z/ho constant (horizontal lines).

IV. DISCUSSION OF RESULTS

A. THE CASE OF DEEPER VORTEX SUBMERGENCE

1. Velocity, Turbulence, and Reynolds Stresses

The coordinate axes and velocities are shown in Figure 1. The axial velocity, normalized by the mean velocity U_o, is shown in Figure 2 for representative values of z/h_o from 0.08 to 1.00 for the vortex situated at ho/Rc = 5.58 at a downstream distance of x/c = 3.00 from the generating airfoil. Figure 2 shows two significantly different regions; one immediately above the vortex where the axial velocity deficit is quite prominent, and the other immediately under the 'scar' where the axial velocity defect is somewhat smaller. Beyond this immediate observation, one notes that the axial velocity defect increases as one approaches the vortex. This is somewhat anticipated on the basis of the fact that the mutual interaction of the circumferential velocities and the axial velocity near the free surface is much smaller than that near the vortex. Below the scar, however, the said variation acquires a new character for two reasons: (a) the induced circumferential velocity at the scar location is smaller than that at the free surface because of its relative distance, and (b) the scar causes further changes in the velocity as well as turbulence characteristics of the flow, as will be noted later. Suffice it to say that the axial velocity variation in the flow map of the transverse cross section is a strong indication of the events to follow.

The variation of the lateral component of the velocity is shown in Figure 3. The most immediate striking feature of the nine velocity profiles is that they reverse their direction, as expected, depending on whether the

measurements are taken above or below the vortex. Immediately above the vortex, and near the free surface, the lateral velocity is fairly flat and increases as one approaches the vortex. Thus, one would expect that the fluid, which is allowed to move mostly in the axial and lateral directions, rather than in the vertical direction, would enhance the occurrence of a scar in the direction away from the $y/Rc = 0$ axis. Compared with the axial component of the velocity, the lateral component does not show a major change at or near the scar. This is primarily because the scar is stationary and the vortex-induced lateral component of the velocity is further diminished by the increased radial distance to the scar.

Further away from the free surface, the variation of the lateral component of the velocity is just as expected, i.e., it follows the typical velocity profile induced by a potential vortex. It should be noted in passing that the smoothness as well as the repeatability of the data speak for the accuracy of the data presented here.

The vertical component of velocity, normalized by U_o, is shown in Figure 4, as positive downward (i.e., in the direction away from the free surface), for eight different values of z/h_o. It is clear that the magnitude of the vertical component of velocity exhibits the usual vortex behavior near the vortex axis and decreases sharply from large (downward) values to small but upward values as one approaches the free surface near the scar ($-10 < y/Rc < -6$). This is in accord with the expectations that the normal component of velocity at or near the free surface should rapidly diminish even though the free surface is not rigid. A closer examination of the data for $z/h_o = 0.08$ in Figure 4 shows that w/U_o is not symmetrical with respect to the vortex axis.

This is primarily due to the fact that the counterclockwise rotation of the vortex leads to the accumulation of the fluid on the left of the free surface and vice versa.

The turbulence intensities u'/U_o ($= \sqrt{u'^2}/U_o$ = Root-Mean-Square value of the u'-component of turbulence normalized by U_o), v'/U_o, and w'/U_o are shown in Figures 5, 6, and 7, in percent, as a function of y/Rc for six representative values of z/ho, all for x/c = 3. In each figure, the turbulence values at y/Rc = 0 are those directly above the vortex axis and the turbulence intensities in the neighborhood of y/Rc = -6 to -10 are those directly below the free-surface scar.

Each turbulence intensity exhibits its unique variation and sheds considerable light on the deformation of the free surface. Figure 5 shows that near the free surface (henceforth called 'the surface layer') u'/U_o above the vortex axis is smaller than in the scar region. However, as z/h_o increases, i.e., as one approaches the vortex core, u'/U_o increases and reaches values as large as those in the scar. Outside the region of the scar and of the vortex core, i.e., for y/Rc smaller than about –12 and larger than about 8, u'/U_o reaches its minimum value. The most important fact, however, is that in the surface layer u'/U_o decreases **above the vortex axis** and **increases in the scar zone.** This is the first important indication of the transfer of turbulent kinetic energy from the vertical to the horizontal components in the axial and lateral directions. In fact, Figures 6 and 7 provide irrefutable evidence of the said transfer of turbulent energy. Figure 6 shows that v'/U_o increases dramatically in the scar zone relative to any other region. In the vicinity of the vortex plane ($0 < y/Rc < 4$) and only at or near the vortex level (z/h_o = 0.63 to 1.00)

that v'/U_o shows a small increase. On the other hand, Figure 7 shows that w'/U_o in the scar zone ($-10 < y/Rc < -6$) is not significantly different from that in the ambient region farther to the left ($y/Rc < -12$). However, w'/U_o above the vortex axis begins with a relatively large value and increases dramatically as the vortex axis is approached. In other words, the turbulence intensities u'/U_o and v'/U_o increase in the scar zone at the expense of w'/U_o. Thus, one may conclude that the nearly isotropic turbulence far below the surface layer is transformed into an anisotropic two-dimensional turbulence by the scar in the surface layer and the energy of the vertical velocity fluctuations is redistributed among the lateral and streamwise motions. Furthermore, all turbulence quantities have strong gradients in the lateral direction in the surface layer. These are some of the most important findings of this investigation. The scar's role in rendering the turbulence anisotropic and rearranging the scales of turbulence eddies is indeed profound since it changes the character of the surface signatures. Thus, the important signature-identification problem reduces to a eddy-structure-identification problem. This issue will be taken up again later following the discussion of additional data.

Figures 8 and 9 show the Reynolds stresses $u'v'$, $u'w'$, and $v'w'$, all normalized by U_o^2, as a function of z/h_o, above the vortex and in the scar zone, respectively. A comparison of the relative magnitudes of these stresses above the vortex shows that (Figure 8) they are of the same order of magnitude, particularly in the layer containing the vortex. The fact that $v'w'$ is somewhat larger than the other two is strictly attributable to the fact that near the vortex core the two turbulence components (v' and w') are much

better cross-correlated relative to the other components because of the coherence of the vortex core as a result of its compact vorticity distribution.

As the free surface is approached, all components of the Reynolds stresses decrease rapidly and there is no prominent Reynolds stress. This is normally what one expect as one approaches a shear-free fluid interface. However, Figure 9 exhibits a strikingly different character and reinforces the conclusions arrived at earlier. Specifically, in the scar zone, the Reynolds stresses u'w' and v'w' are negligibly small, because there does not exist a vortex-like coherent structure to enhance the cross correlation between w' and the other two components. However, the u'v' component of the Reynolds stress is large not only at the vortex level but throughout the entire region below the scar zone. No better convincing or corroborating evidence can be provided than the data shown in Figure 9 that the turbulence in the scar zone of the surface layer has become two-dimensional, i.e., anisotropic, and that this anisotropy is not uniform across the surface layer; it has gradients on both sides of the scar. It is this gradient that sorts out the integral length scales of turbulence and the size of the identifiable structures.

It is a fitting summary to the discussion of the velocities, turbulence intensities, and Reynolds stresses that all kinematic characteristics of flow in the scar zone are strongly affected by the formation of the scar to an extent distinctly different from any other region in the flow or in the surface layer. Thus, it remains to be determined as to how the energy in that region is distributed among the various scales of turbulence.

2. Energy Spectra

Figures 10 through 12 show the energy spectra E_u, E_v, and E_w for the three components of turbulence as a function of the frequency for various values of z/h_o, along a line directly above the vortex. The smaller frequencies correspond to larger eddy structures and vice versa. A quick comparison of these figures show that (a) the magnitudes of E_u, E_v, and E_w decrease in the order the spectra are listed, i.e., E_w is about an order of magnitude smaller than E_v, and E_v is about two orders of magnitude smaller than E_u, and (b) all spectra decrease, to varying extent, with increasing frequency, but the rate of decrease of E_u is much stronger than that of E_v, and the rate of decrease E_v is somewhat larger than that of E_w. In fact, the change in E_w with frequency is almost imperceptible, showing that the energy in the z-component of turbulence is almost uniformly distributed among the scales displayed. On the other hand, at the high frequency end, the E_u component follows a –5/3 power law, implying that in the region of nearly isotropic turbulence, the E_u-spectra follows Kolmogorov's decay law of the inertial sub-range and that the interaction of the vortex generated turbulence with the free surface is confined to relatively small frequencies or large eddy scales in the surface-influenced layer.

The spectra measurements thus show that in the surface-influenced layer **above the vortex** the partition of the energy among the three components of turbulence is such that the u-component contains most of the energy at the larger structures and decays rapidly at the smaller scales. The v-component contains smaller energy at all scales even though the larger structures have a slightly larger energy and decay much slower. Finally, the

w-component of energy is small at all scales and shows no appreciable change throughout the frequency domain exhibited in Figure 12.

Figures 13 through 15 show the energy spectra E_u, E_v, and E_w for the three components of turbulence as a function of the frequency for various values of z/h_o, along a vertical line **bisecting the scar zone**. The smaller frequencies correspond to larger eddy structures and vice versa. A quick comparison of these figures show, as before, that (a) the magnitudes of E_u, E_v, and E_w decrease in the order the spectra are listed, i.e., E_w is about an order of magnitude smaller than E_v, and E_v is about two orders of magnitude smaller than E_u, and (b) all spectra decrease, to varying extent, with increasing frequency, but the rate of decrease of E_u is much stronger than that of E_v, and the rate of decrease of E_v is somewhat larger than that of E_w.

As before, the E_u component nearly follows a $-5/3$ power law at higher frequencies. However, E_u in the scar zone (Figure 13) is almost an order of magnitude larger than E_u in the surface layer above the vortex (Figure 10), particularly at lower frequencies or for larger scales. In other words, scar is a scale, energy, and isotropy transformer. It helps to transfer energy from the vertical to horizontal components, from smaller to larger scales, and from nearly isotropic to almost anisotropic turbulence. The order of magnitudes and the rates of decay of the power spectra show that the typical turbulence eddies elongate along the x axis, shorten along the y axis and flatten along the z axis, resembling, in the final analysis, an ellipse-shaped pancake. All the measurements reported above for the deeply submerged vortex attest to this fact.

B. THE CASE OF SHALLOWER VORTEX SUBMERGENCE

1. Velocity, Turbulence, and Reynolds Stresses

Normalized as before, the axial velocity is shown in Figure 16 for representative values of z/h_o from 0.21 to 2.07 for the vortex situated at ho/Rc = 1.15 at a downstream distance of x/c = 3.00 from the generating airfoil. Figure 16 shows, as in the case of deeper submergence, two significantly different regions; one immediately above the vortex where there is an axial velocity defect, and the other immediately under the 'scar' ($-4 < y/Rc < -2$) where there is in fact an axial velocity excess. Beyond this immediate observation, one notes that the axial velocity defect increases as one approaches the vortex. This is somewhat anticipated on the basis of the fact that the mutual interaction of the circumferential velocities and the axial velocity near the free surface is smaller than that near the vortex. Below the scar, however, the said variation acquires a new character for three reasons: (a) the induced circumferential velocity at the scar location is smaller than that at the free surface because of its relative distance, and (b) the scar causes further changes in the velocity as well as turbulence characteristics of the flow, as noted earlier, and (c) the proximity of the vortex to the free surface spreads the vorticity of the vortex over a larger area (as seen by extensive visual observations). A closer examination of Figure 16 in the scar zone shows that very near the free surface (z/ho = 0.21) there is practically no axial velocity excess or deficit.

The lateral component of the velocity is shown in Figure 17. The most immediate striking feature of the six velocity profiles is that v/U_o is

nearly zero above the vortex and acquires small positive values in the scar zone. This is expected on the basis of earlier discussions that the occurrence of scar enhances the energy transfer to axial and lateral directions.

The vertical component of velocity is shown in Figure 18, as positive downward (i.e., in the direction away from the free surface), for seven different values of $z/h_{o.}$. It is clear that the magnitude of the vertical component of velocity exhibits the usual vortex behavior near the vortex axis and decreases sharply from large (downward) values to nearly zero as one approaches the free surface. A closer examination of the data for $z/h_o = 0.21$ in Figure 18 shows that w/U_o is rather small but downward in the scar zone. This is unlike the deeper submergence case and is attributed to the distribution of vorticity over a larger area. In any case, the magnitude of w/U_o is in the order of the rms value of turbulence in the scar zone and the upward or downward fluctuations in the velocity should be attributed partly to the free-surface fluctuations due to turbulence (small whirls, waves, striations, etc.) and partly to the difficulty of making velocity and turbulence measurements very near a dynamic free surface.

The turbulence intensities u'/U_o v'/U_o, and w'/U_o are shown in Figures 19, 20, and 21, in percent, as a function of y/Rc for seven representative values of z/ho. In each figure, the turbulence values at y/Rc = 0 are those directly above the vortex axis and the turbulence intensities in the neighborhood of $-4 < y/Rc < -2$ are those directly below the free-surface scar.

Each turbulence intensity exhibits its unique variation and sheds considerable light on the deformation of the free surface. Figure 19 shows that near the free surface u'/U_o above the vortex axis is somewhat larger than

in the scar region. This is primarily due to the extreme proximity of the vortex to the free surface and the strong deformation of the vortex core. Figure 20 shows that the v'-component of turbulence is almost flat throughout the surface-influenced layer regardless of the lateral position of the point of measurement. Finally, Figure 21 shows that directly above the vortex axis w'/U_o is relatively large due to the rising of the surface directly above the vortex and diminishes rapidly as one approaches the scar zone. Clearly, the u' and w'-components of turbulence have strong gradients in the lateral direction in the surface layer. These are some of the most important consequences of the extreme proximity of a vortex to a free surface. They show clearly that the velocity and turbulence near the free surface depend not only on the particular region (scar zone or the region directly above the vortex) but also and strongly on the proximity of the vortex to the free surface. In more specific terms, the 'proximity' effect will have to be translated into the shape of the vortex and the distribution of vorticity in that vortex. The scar zone created by a deeply submerged coherent vortex and the ensuing velocity and turbulence field are not expected to be identical to those created by a vortex in the immediate vicinity of the free surface. It follows that the consequences of a compact vortex, generated at great depths and migrating towards the free surface, are significantly different from those of a turbulent wake, generated by a propeller, containing large amounts of non-coherent vorticity. In either case, the scar's role in rendering the turbulence anisotropic and in rearranging the scales of turbulence eddies, i.e., the physics of the flow, remain fundamentally the same. However, the magnitude of the resulting physical parameters change. When the vortex is very close the free

surface, the deformations directly above the vortex center (more specifically, the distributed vorticity zone) predominate those in the scar zone, the scar and other free-surface deformations become intermingled and form a highly-deformed surface-influenced layer. When the vortex is deeply submerged, the characteristics of the scar stand out since the direct influence of the vortex on the surface immediately above the vortex axis is indeed negligible. Suffice it to note that, with deep submergence, the outstanding features of the scar are not obscured by those of the vortex. With shallower submergence, the two effects become indistinguishably intermingled. In other words, the surface signatures resulting from an ascending vortex generated by a submarine are bound to be significantly different from those generated by the wake of a surface ship. Thus, the important signature-identification problem reduces to an eddy-structure-identification problem as noted earlier. The important fact is that the differences in scar structure lead to the identification of the character of the sources which gave rise to them.

Figures 22 and 23 show the Reynolds stresses u'v', u'w', and v'w', all normalized by U_o^2, as a function of z/h_o, above the vortex and in the scar zone, respectively. A comparison of the relative magnitudes of these stresses above the vortex shows that (Figure 22) they are uniformly small everywhere and of the same order of magnitude, particularly in the layer containing the vortex. The fact that v'w' is somewhat larger than the other two is strictly attributable to the fact that near the vortex core the two turbulence components (v' and w') are much better cross-correlated relative to the other components because of the semi-coherent character of the vortex near its mathematical center of vorticity.

As the free surface is approached, all components of the Reynolds stresses decrease rapidly and there is no prominent Reynolds stress. As noted earlier, this is normally what one would expect as one approaches a shear-free fluid interface. However, Figure 23 exhibits a strikingly different character and reinforces the conclusions arrived at in the case of deeper vortex submergence. Specifically, in the scar zone, the Reynolds stresses u'w' and v'w' are negligibly small, because there does not exist a vortex-like structure, let alone a coherent one to enhance the cross correlation between w' and the other two components of turbulence. However, the u'v' component of the Reynolds stress is large not only at the vortex level but throughout the entire region below the scar zone. This confirms the earlier assertions that the turbulence in the scar zone of the surface layer has become two-dimensional, i.e., anisotropic, and that this anisotropy is not uniform across the surface layer; it has gradients on both sides of the scar. It is this gradient that sorts out the character, the integral length scales of turbulence, and the size of the identifiable structures.

In summary, the velocities, turbulence intensities, and Reynolds stresses show once again that all kinematic characteristics of flow in the scar zone are strongly affected by the formation of the scar. However, the proximity and the diffused nature of the vortex tends to obscure the predominance of the scar in the case of shallow submergence of the vortex. This gives rise to the distinct differences between the structures created by coherent structures migrating towards the free surface (as in the case of submarine vortices) and those created by turbulent wakes (as in the case of ship wakes) which are already in the surface zone.

2. Energy Spectra

Figures 24 through 26 show the energy spectra E_u, E_v, and E_w for the three components of turbulence as a function of the frequency for various values of z/h_o, along a line directly above the vortex. A quick comparison of these figures show that (a) the magnitudes of E_u, E_v, and E_w decrease in the order the spectra are listed, i.e., E_v and E_w are of the same order of magnitude and both are about two orders of magnitude smaller than E_u and (b) all spectra decrease, to varying extent, with increasing frequency, but the rate of decrease of E_u is much stronger than that of others. In fact, the change in E_w with frequency is almost imperceptible, showing that the energy in the z-component of turbulence is almost uniformly distributed among the scales displayed. On the other hand, at the high frequency end, the E_u component follows approximately a –5/3 power law, implying that in the region of nearly isotropic turbulence, the E_u-spectra follows Kolmogorov's decay law of the inertial sub-range and that the interaction of the vortex generated turbulence with the free surface is confined to relatively small frequencies or large eddy scales, particularly in the axial direction in the surface-influenced layer.

All spectra measurements thus show that in the surface-influenced layer **above the vortex** the partition of the energy among the three components of turbulence is such that the u-component contains most of the energy at the larger structures and decays rapidly at the smaller scales. The v- and w-components contain smaller energy at all scales.

Figures 27 through 29 show the energy spectra E_u, E_v, and E_w for the three components of turbulence as a function of the frequency for various

values of z/h_o, along a vertical line **bisecting the scar zone**. They are nearly identical to those shown in Figures 24 through 26 for the corresponding values of the spectrum. This is somewhat expected on the basis of earlier observations that when a relatively incoherent vortex is very near the free surface the influence of the scar is obscured by the structures arising from the vortex directly above it. Thus, one would not anticipate significant differences between the spectra of the scar zone and that of the rest of the surface-influenced layer. All the measurements reported above for the case of shallow submergence attest to this fact.

IV. CONCLUSIONS

The interaction of a single turbulent trailing vortex with a deformable free surface has been undertaken for the quantitative as well as qualitative exploration of the resulting flow field through the measurement of the velocity and turbulence distributions, the analysis of the energy spectra, and the observation of the coherent structures. The evidence presented herein warranted the following conclusions:

1. There are fundamental differences between the velocity, turbulence, and spectral characteristics of the surface/vortex interaction resulting from coherent vortices (as in the case of submarine vortices) and those resulting from relatively incoherent structures (as in the case of ship wakes).

2. There are two regions wherein one the turbulent kinetic energy decays rapidly with increasing vertical distance, and in the other, very near the free surface (in the order of millimeters), the said energy remains essentially constant. The energy of the vertical velocity fluctuations is redistributed among the lateral and streamwise motions.

3. The velocity, turbulence, and energy distributions in the surface-influenced layer are subjected to strong lateral gradients. These help to grade the integral length scales of turbulence and the structure identification.

4. The typical eddies begin as nearly spherical bodies at large depths and transform into pancake-like structures (elongated in the streamwise direction and highly flattened in the vertical direction) as they approach the surface-influenced layer. The lateral gradation of the size and shape of the

typical eddies depend on the energy source (coherent vortex or wake) and on their proximity to the free surface.

5. The use of a turbulent vortex near the free surface of an otherwise smooth uniform flow proved to be a 'kernel' experiment towards the elucidation of the dynamical processes in vorticity/free-surface interaction.

6. Additional measurements of velocity and all components of the Reynolds stress tensor are needed at other stations downstream from the generating foil partly for the understanding of the axial decay of the flow structures and the associated turbulence intensities and partly for the development of a predictive model of the vorticity/free-surface interaction. These measurements and the understanding of the character of the quasi-coherent structures near the free surface constitute the essence of the on-going investigation.

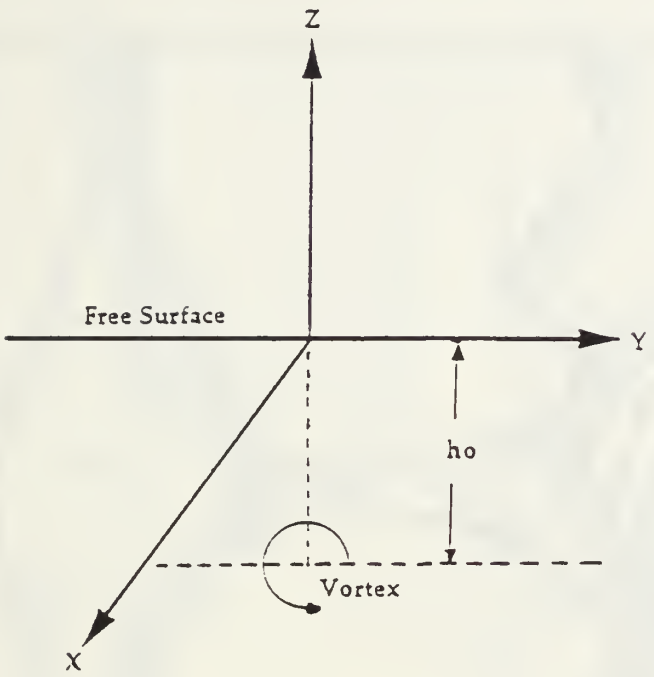

Figure 1. Definition Sketch

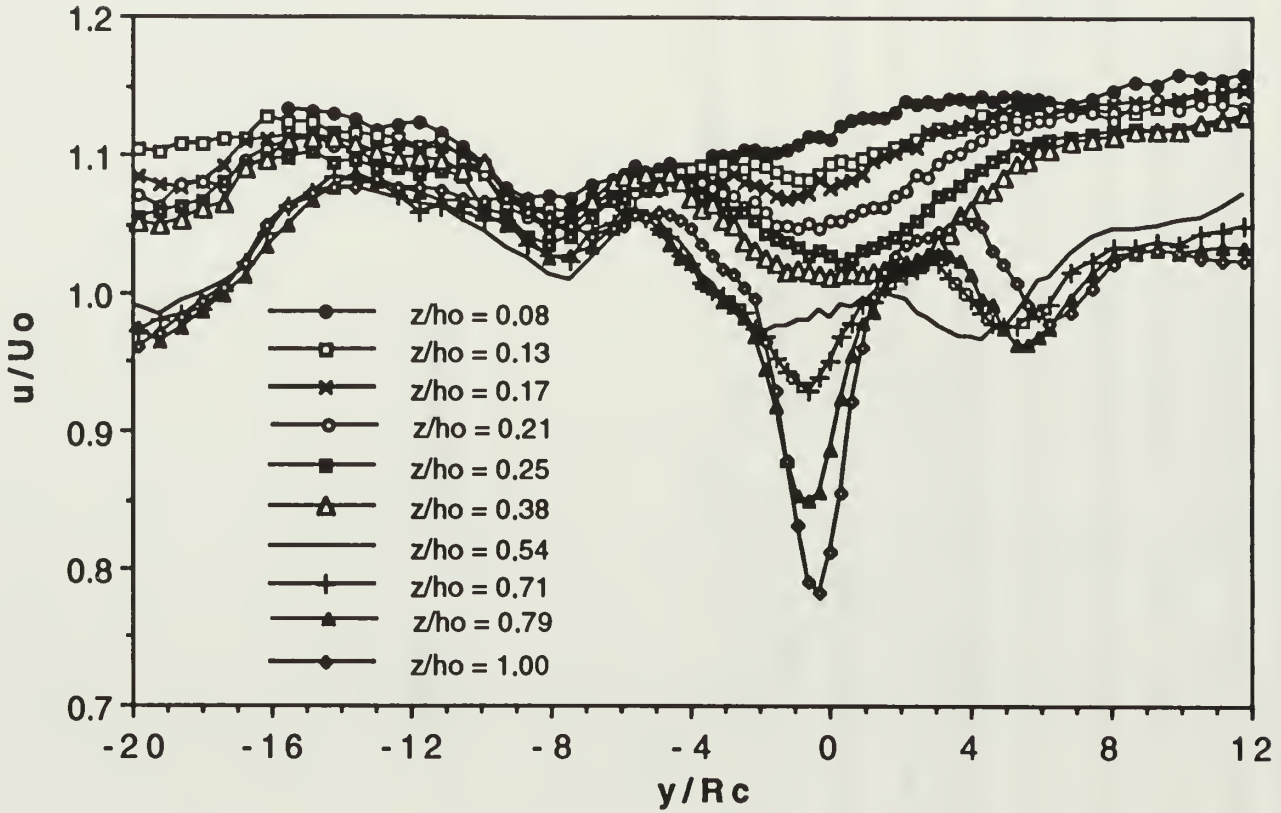

Figure 2. u/Uo versus y/Rc for vortex depth of ho/Rc = 5.58 below the free surface

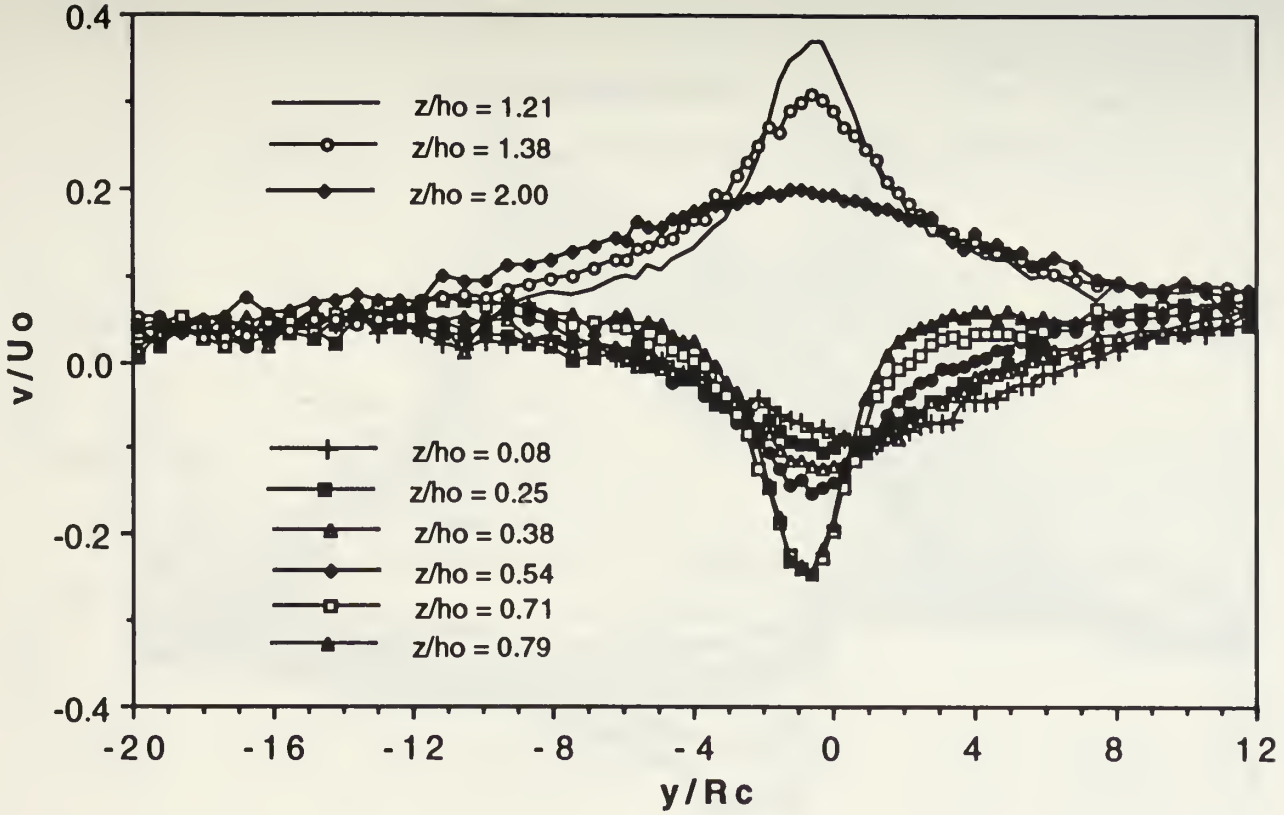

Figure 3. v/Uo versus y/Rc for vortex depth of ho/Rc = 5.58 below the free surface

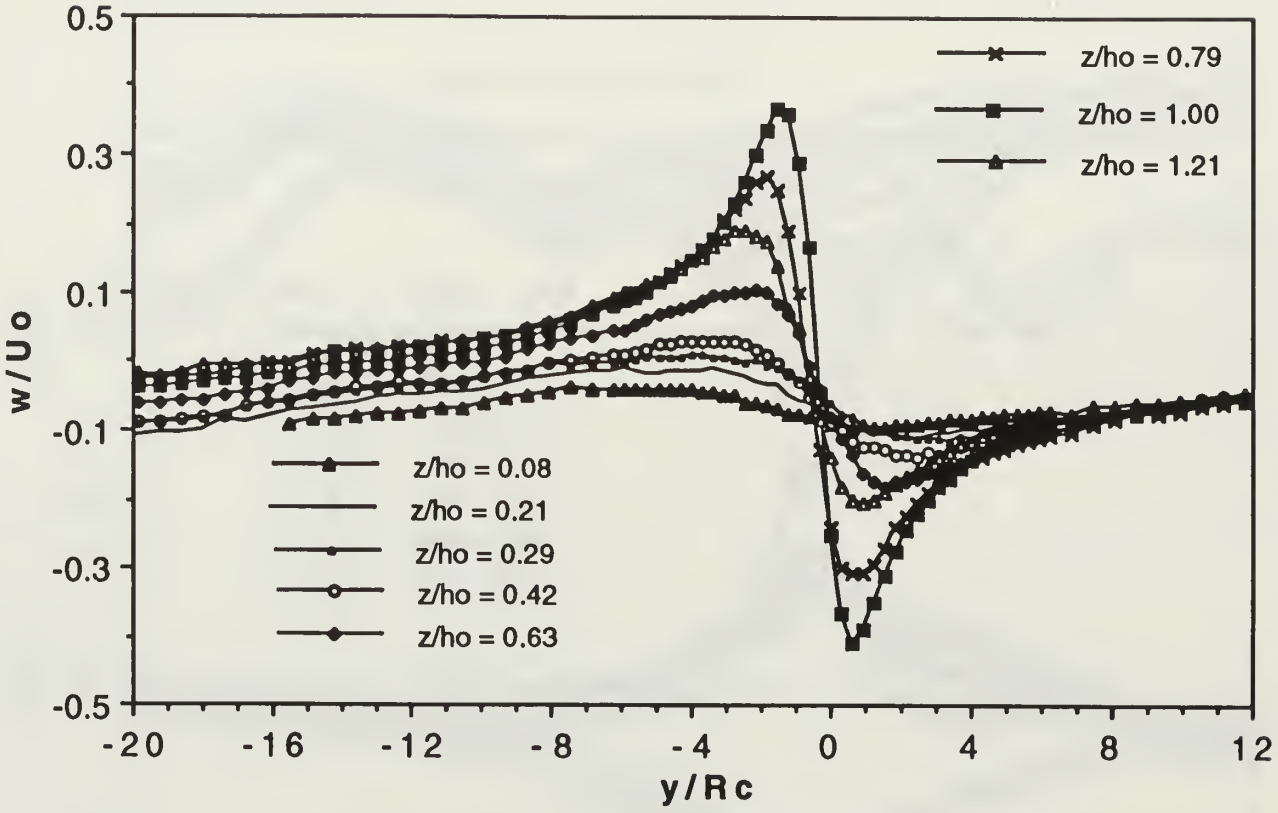

Figure 4. w/Uo versus y/Rc for vortex depth of ho/Rc = 5.58 below the free surface

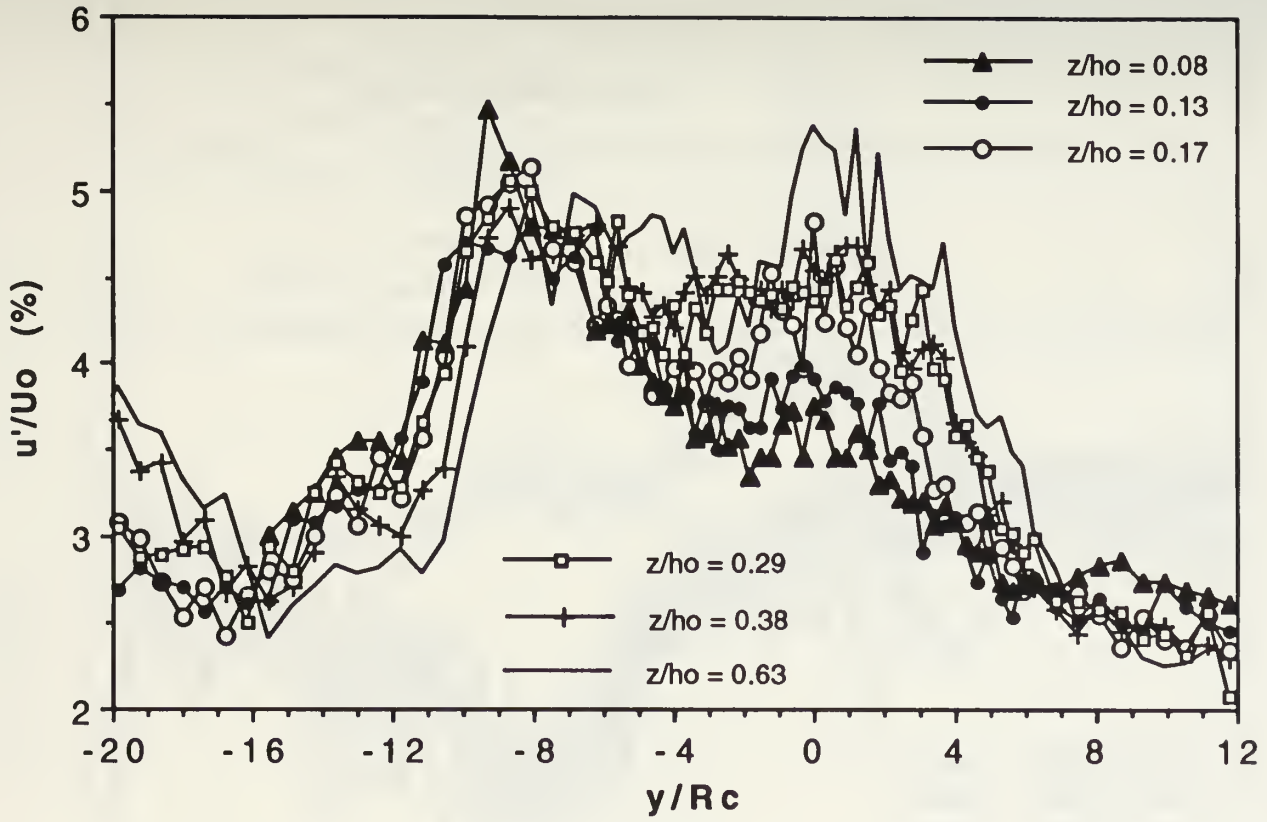

Figure 5. u'/Uo (%) versus y/Rc for vortex depth of ho/Rc = 5.58 below the free surface

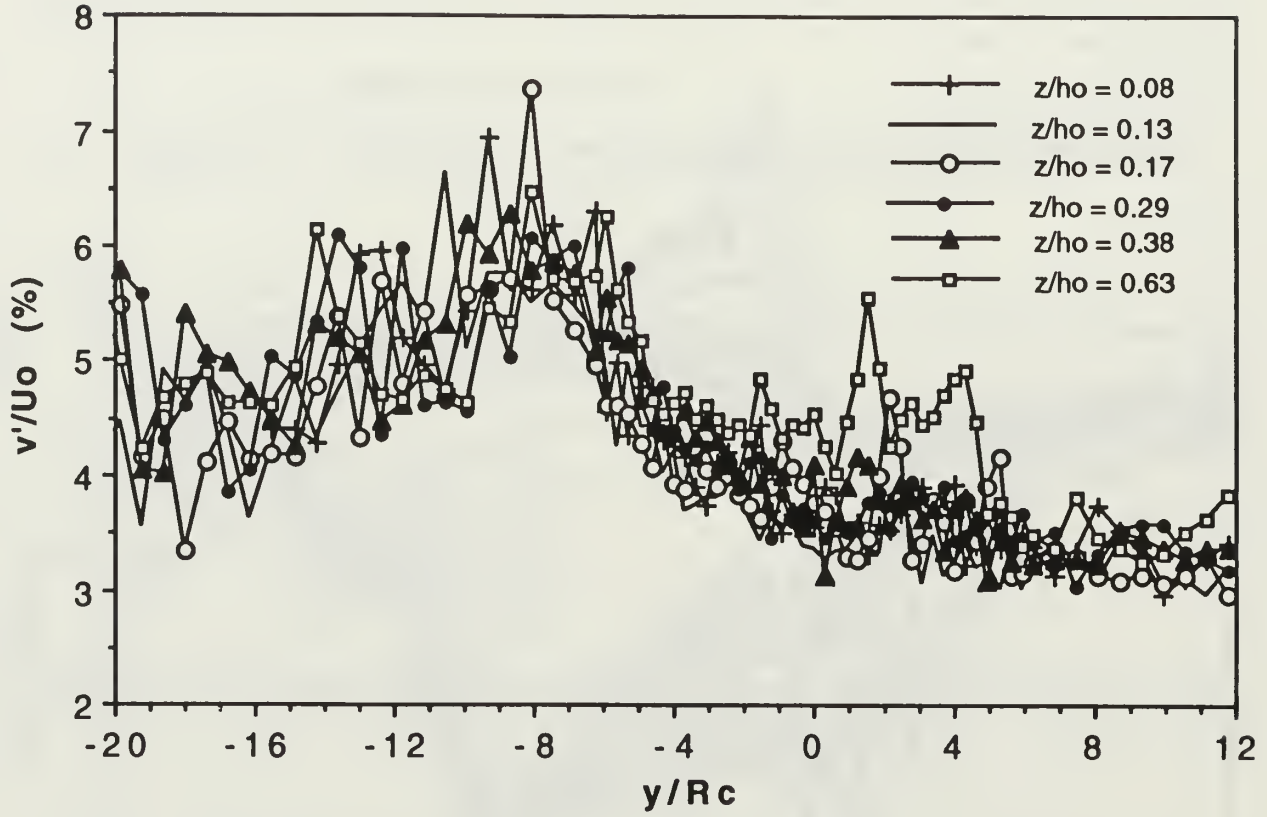

Figure 6. v'/Uo (%) versus y/Rc for vortex depth of ho/Rc = 5.58 below the free surface

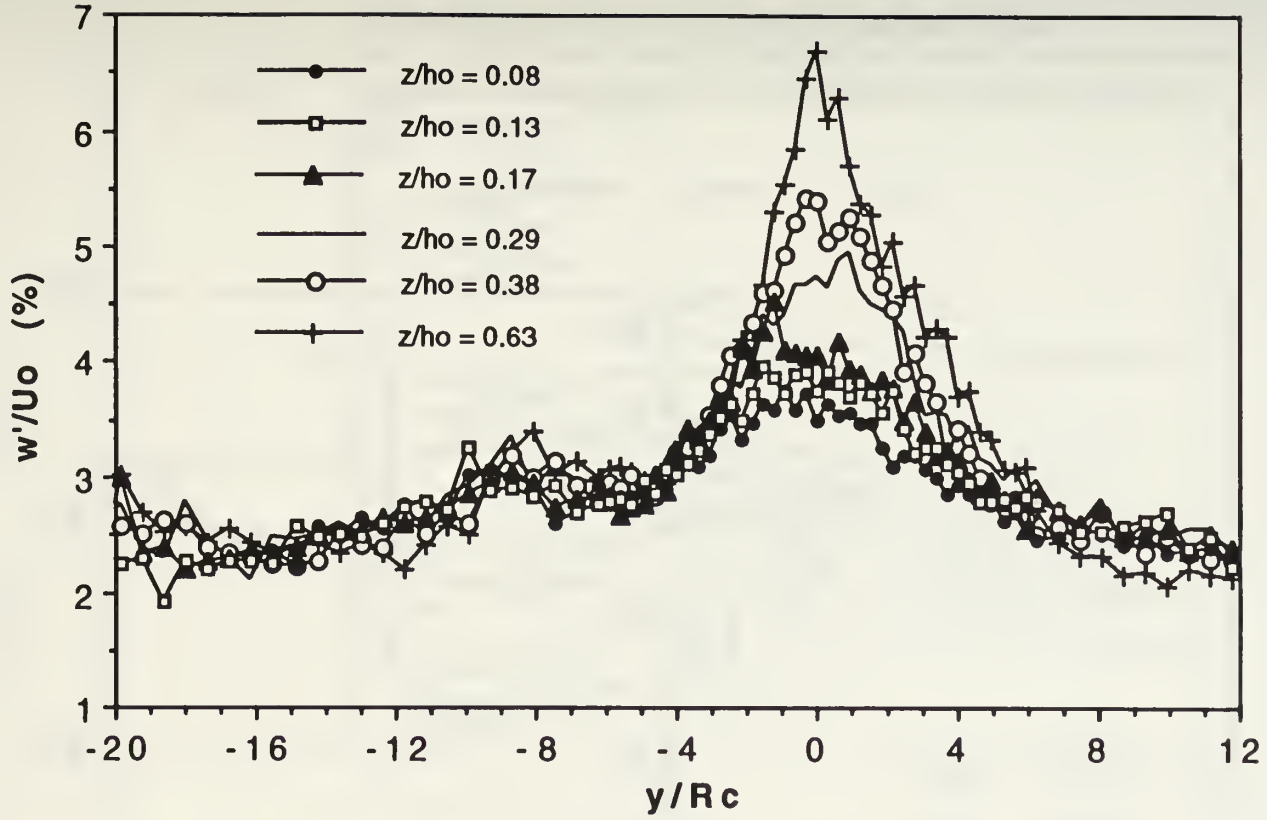

Figure 7. w'/Uo (%) versus y/Rc for vortex depth of ho/Rc = 5.58 below the free surface

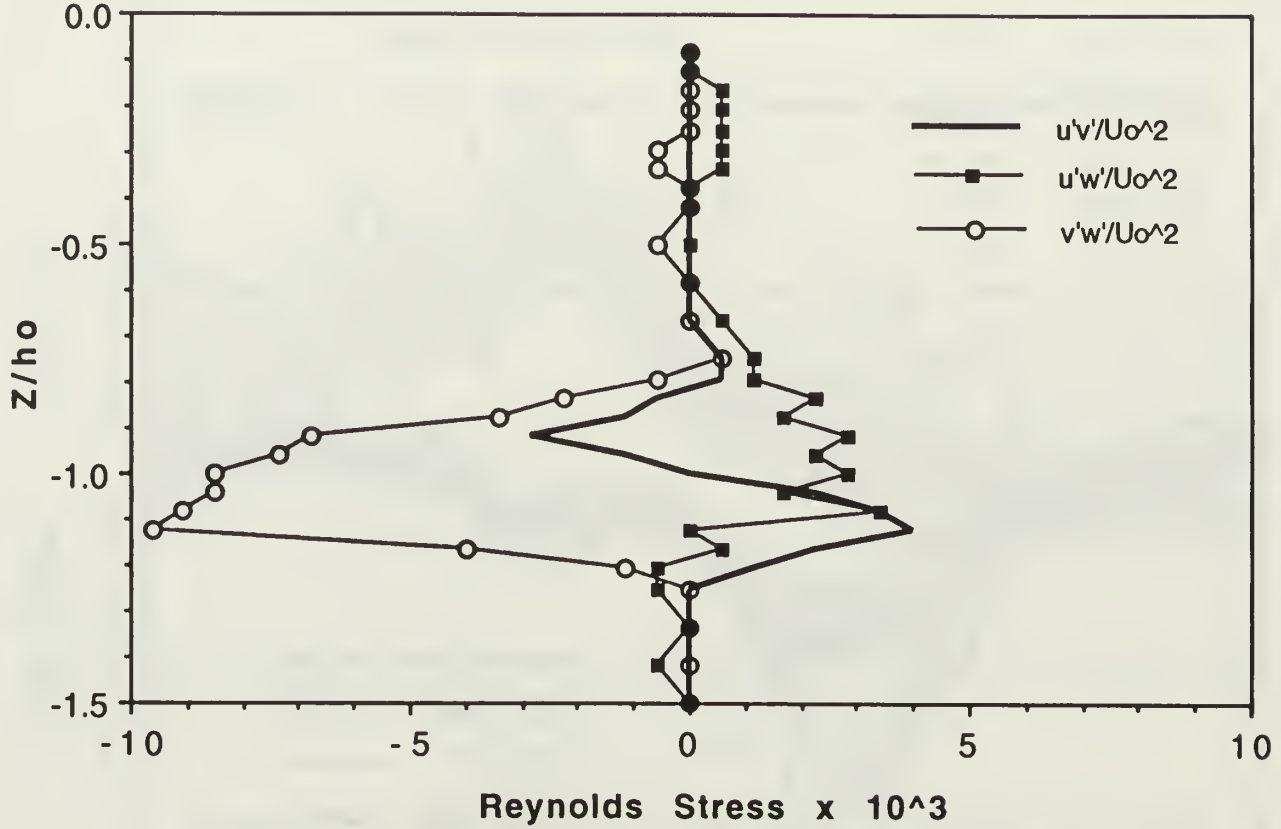

Figure 8. Reynolds Stresses versus z/ho above the vortex centered at a depth of ho/Rc = 5.58 below the free surface

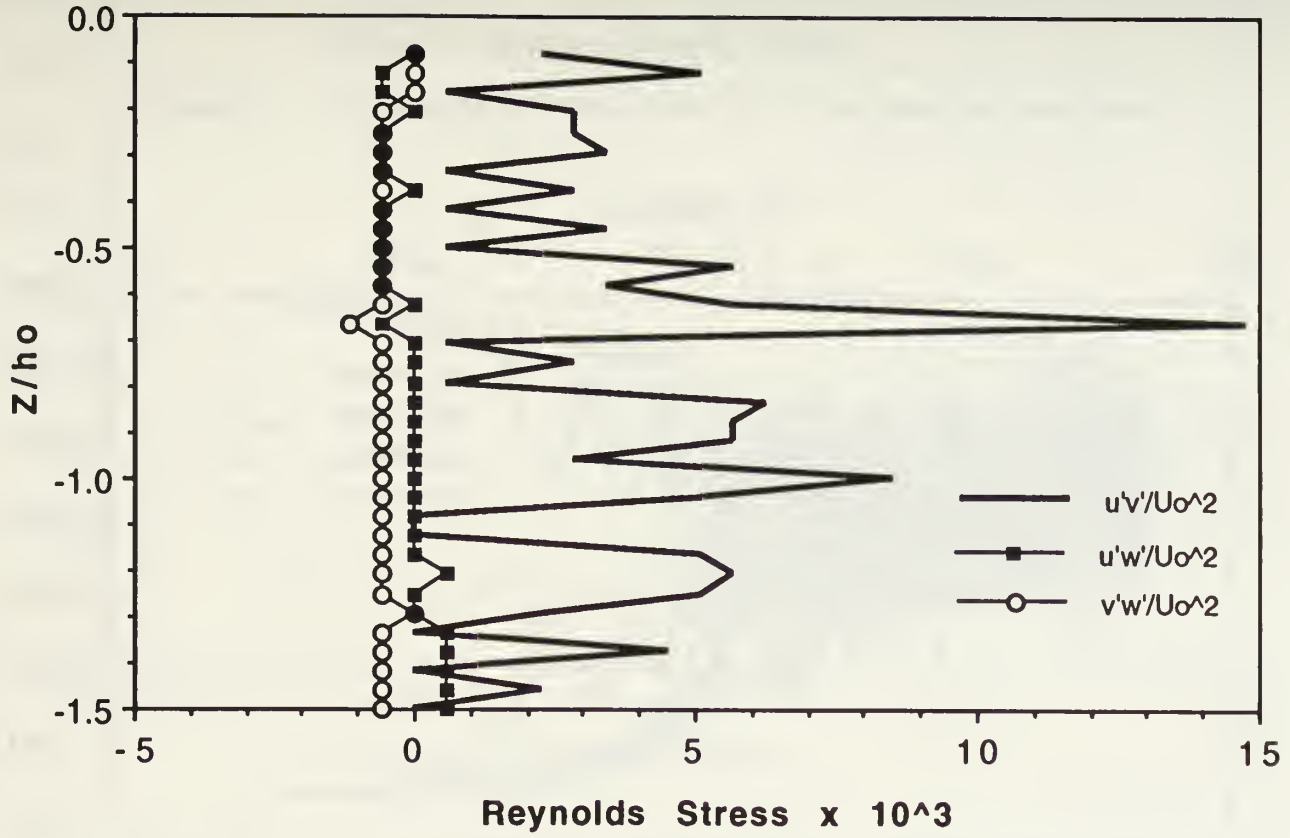

Figure 9. Reynolds Stresses versus z/ho at y/Rc = –7.91 from the vortex centered at a depth of ho/Rc = 5.58 below the free surface

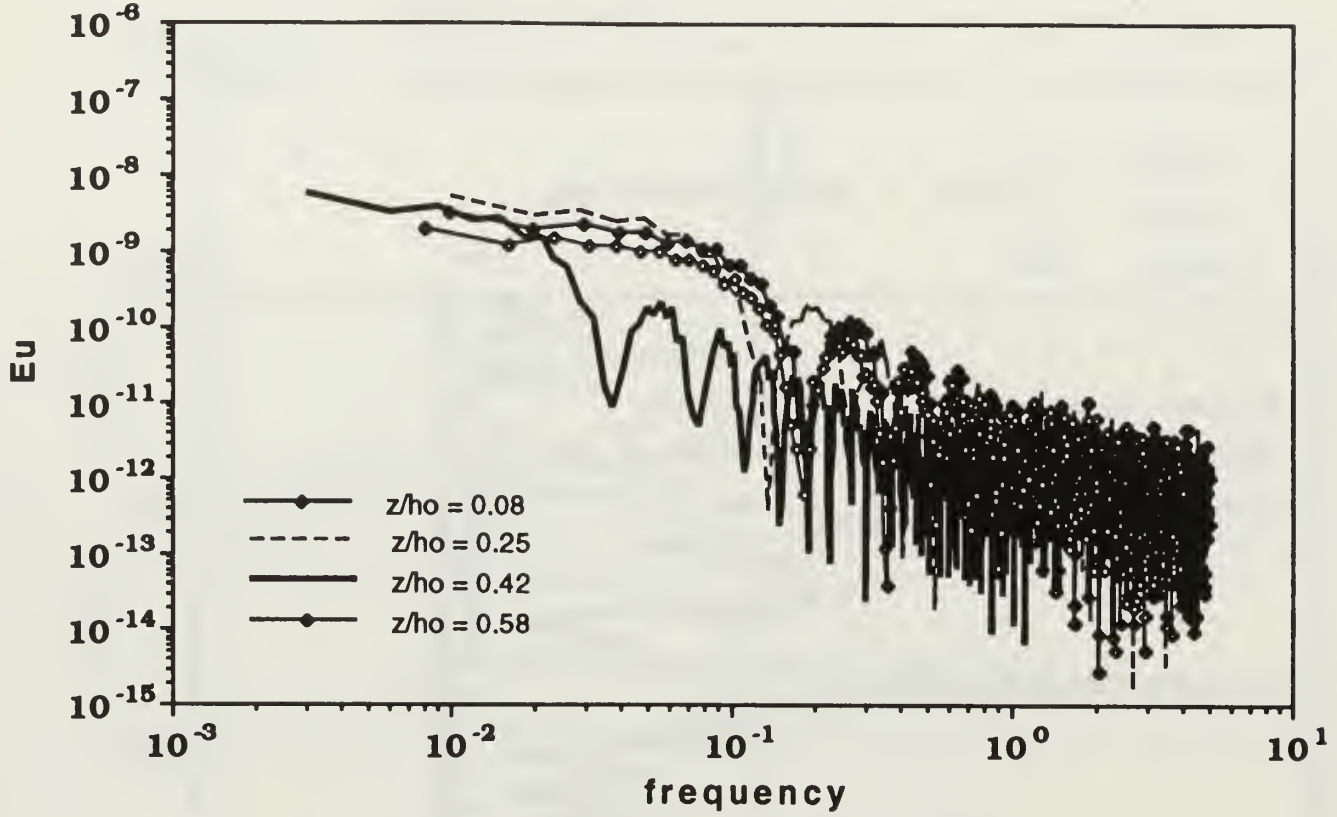

Figure 10. Eu versus Frequency above the vortex centered at a depth of ho/Rc = 5.58 below the free surface

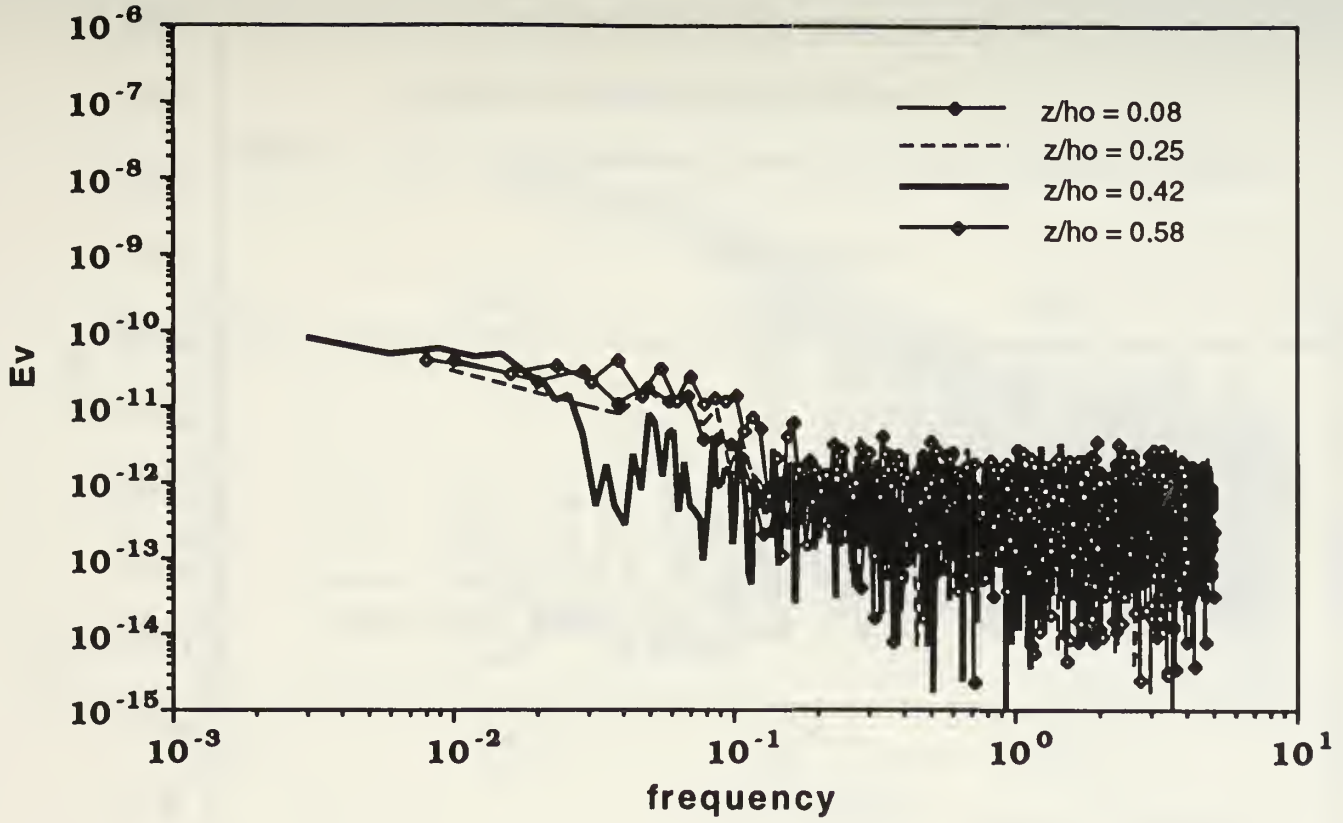

Figure 11. Ev versus Frequency above the vortex centered at a depth of ho/Rc = 5.58 below the free surface

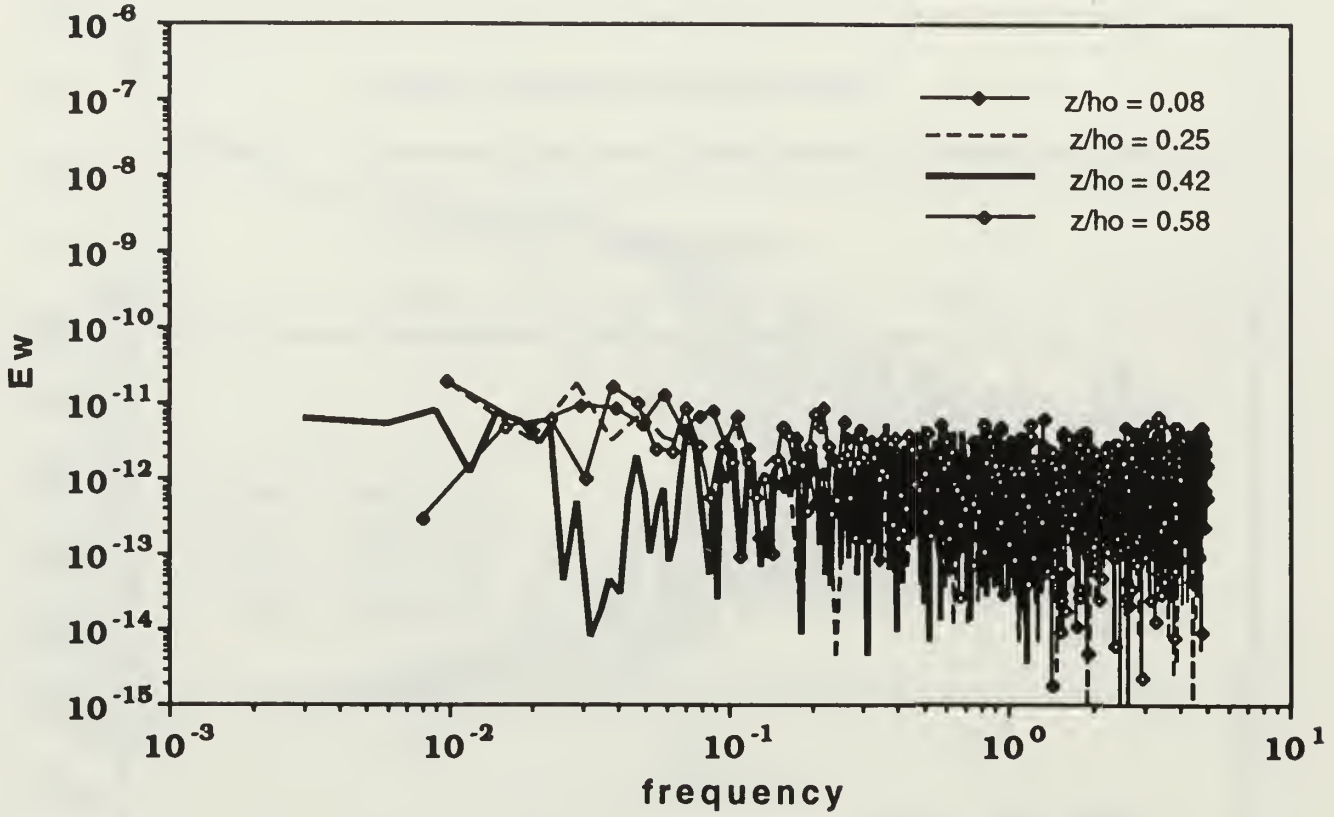

Figure 12. Ew versus Frequency above the vortex centered at a depth of ho/Rc = 5.58 below the free surface

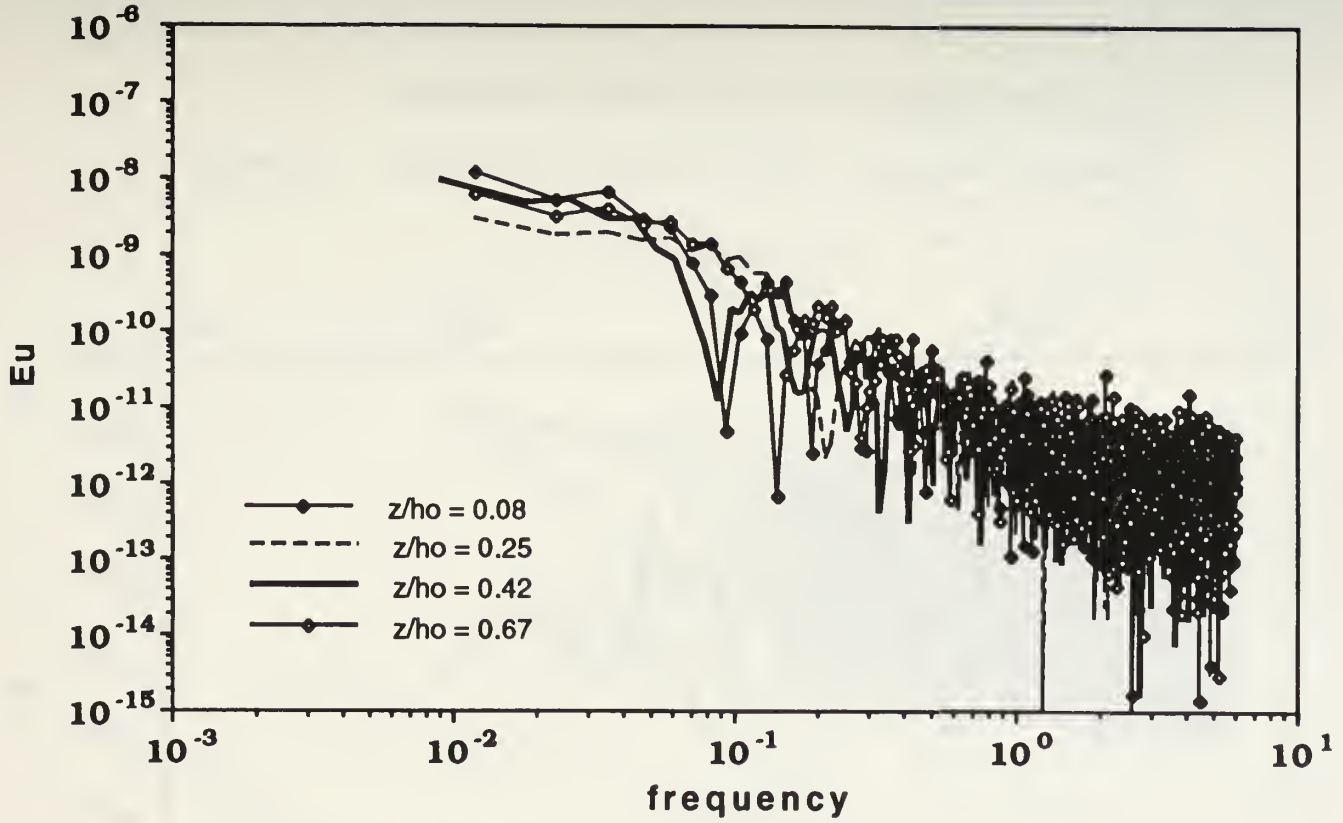

Figure 13. Eu versus Frequency at y/Rc = –7.91 from the vortex centered at a depth of ho/Rc = 5.58 below the free surface

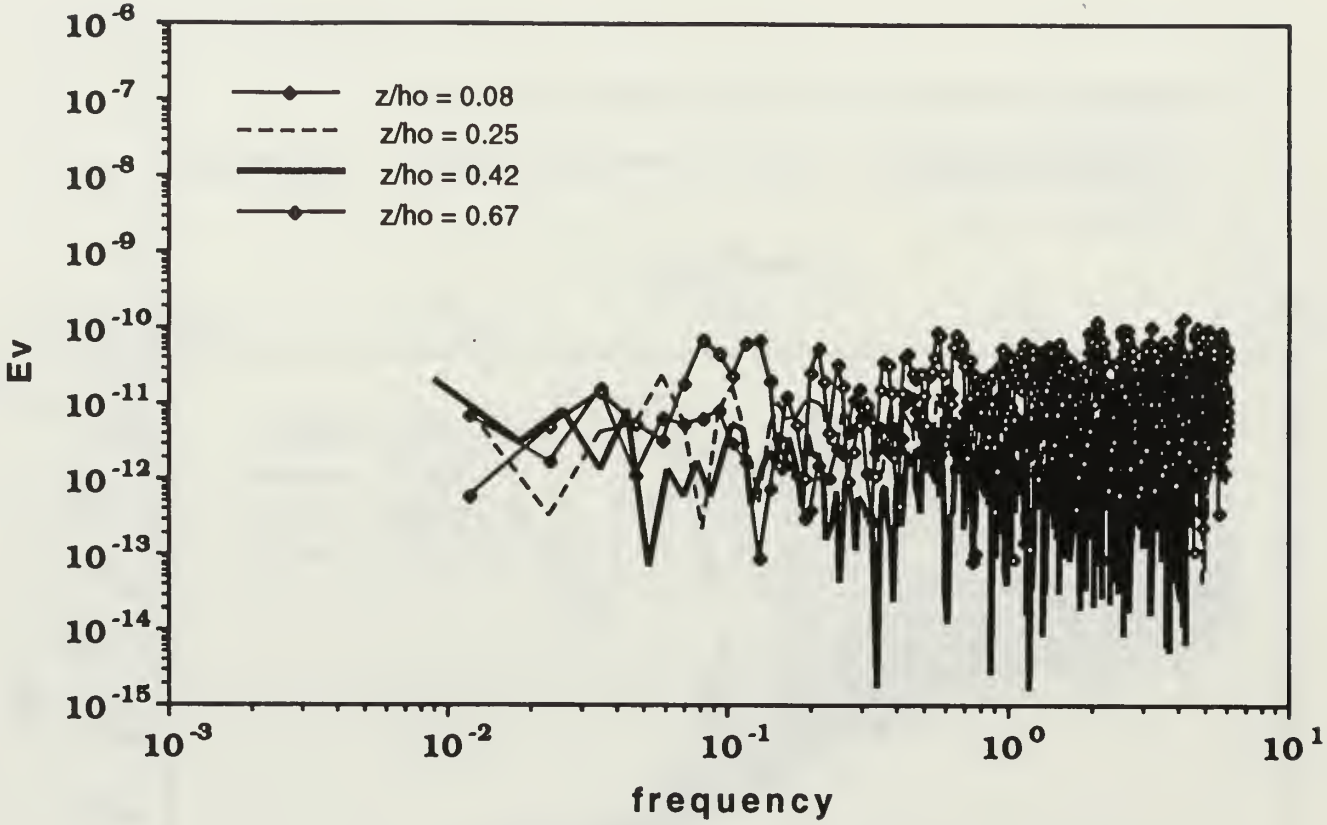

Figure 14. Ev versus Frequency at y/Rc = –7.91 from the vortex centered at a depth of ho/Rc = 5.58 below the free surface

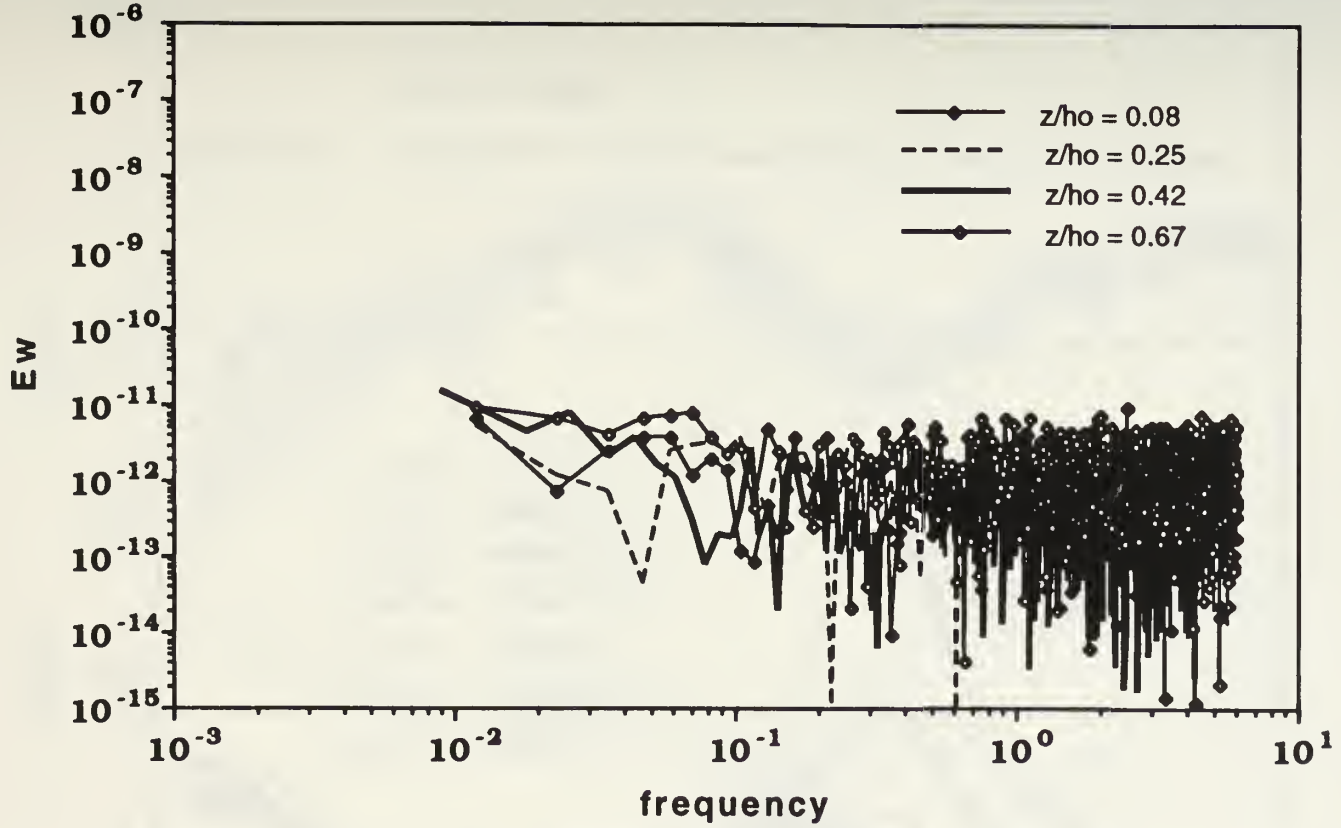

Figure 15. Ew versus Frequency at y/Rc = –7.91 from the vortex centered at a depth of ho/Rc = 5.58 below the free surface

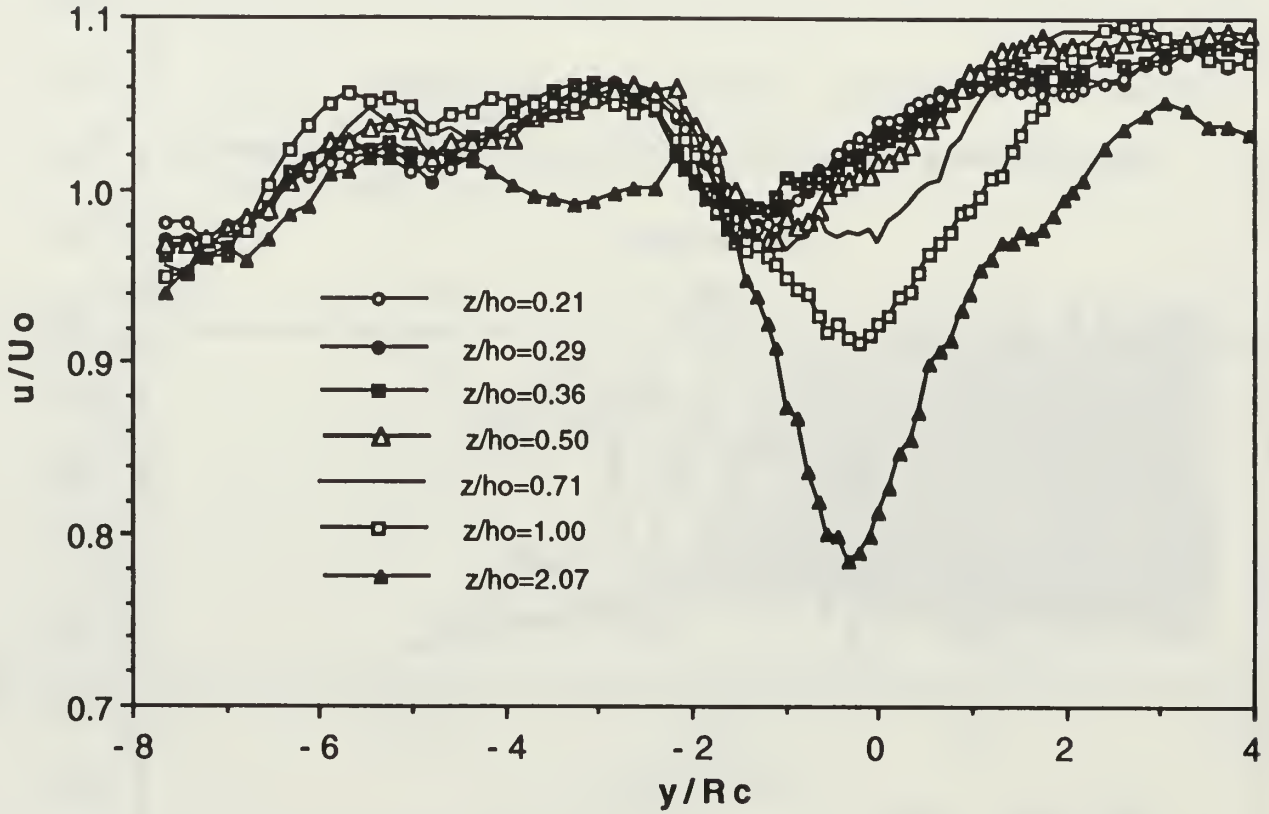

Figure 16. u/Uo versus y/Rc for vortex depth of ho/Rc = 1.15 below the free surface

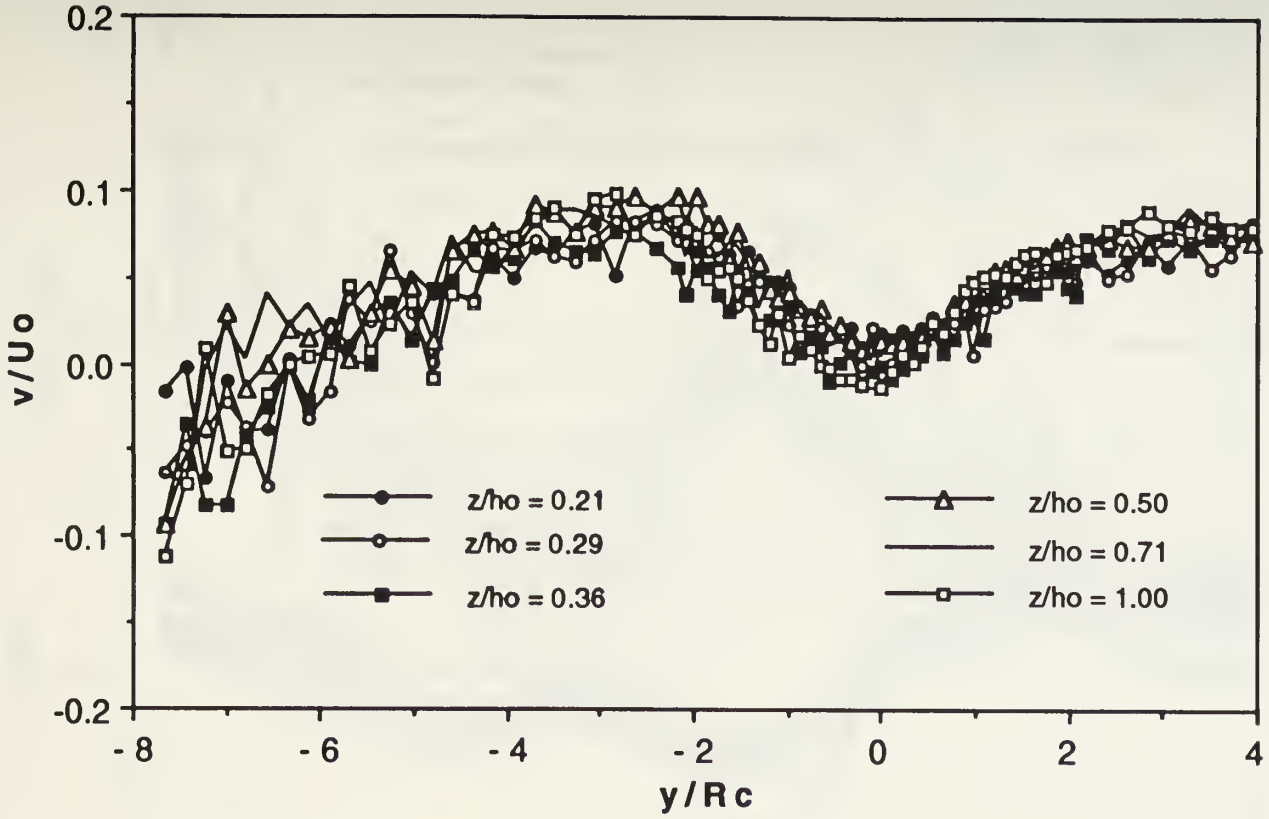

Figure 17. v/Uo versus y/Rc for vortex depth of ho/Rc = 1.15 below the free surface

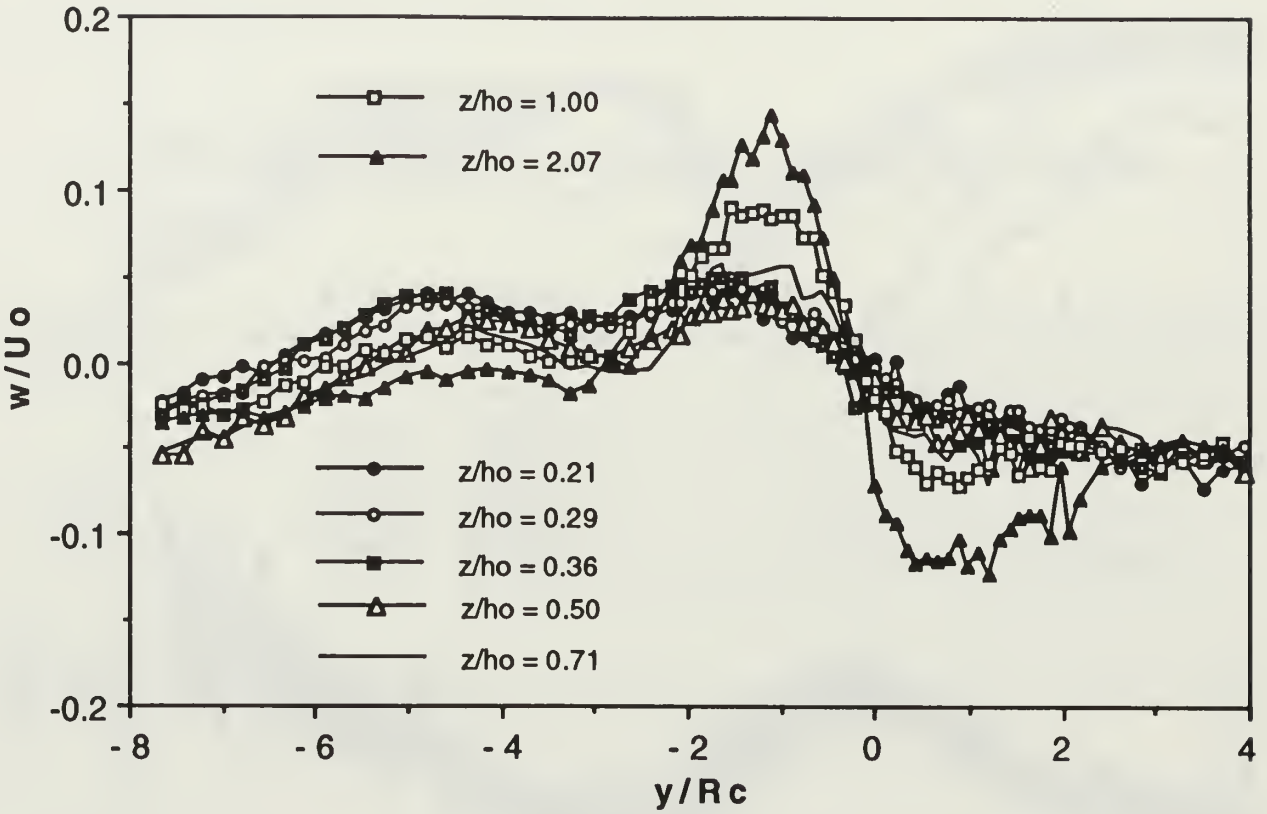

Figure 18. w/Uo versus y/Rc for vortex depth of ho/Rc = 1.15 below the free surface

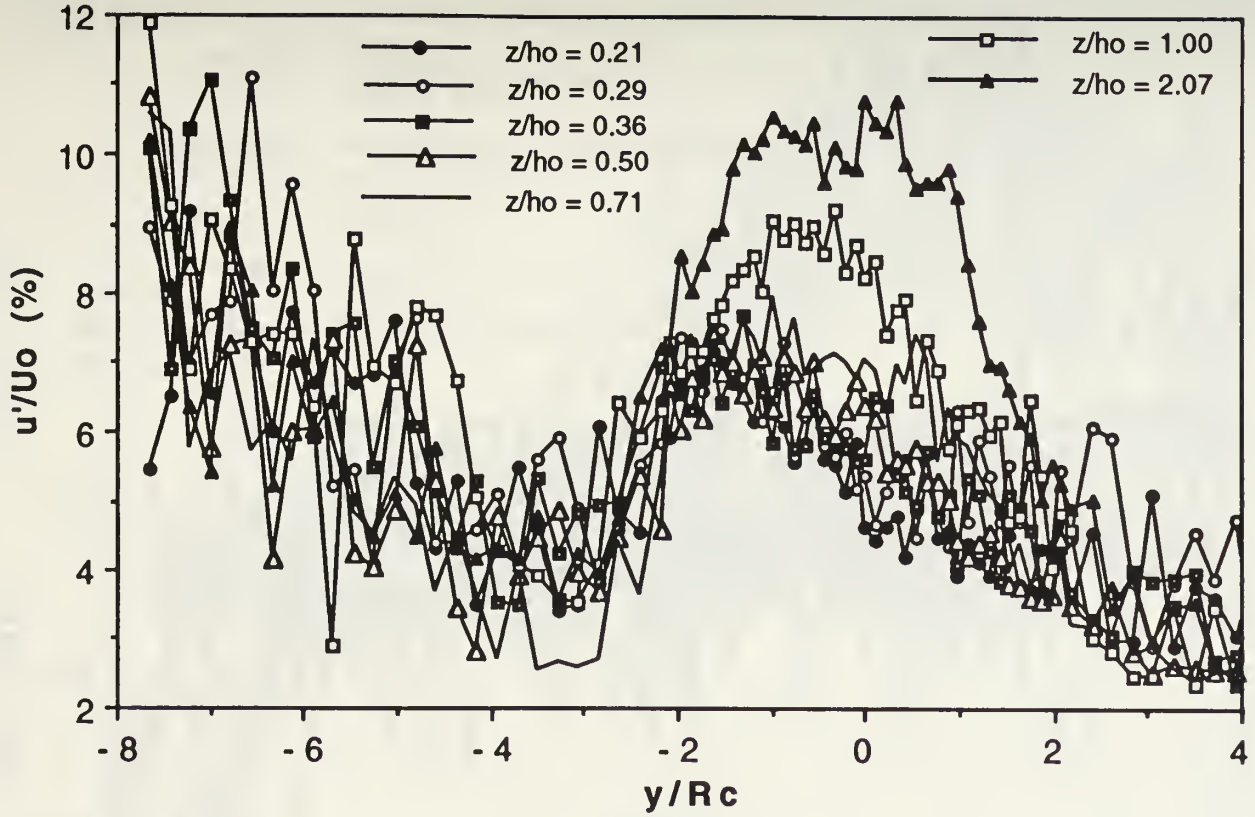

Figure 19. u'/Uo (%) versus y/Rc for vortex depth of ho/Rc = 1.15 below the free surface

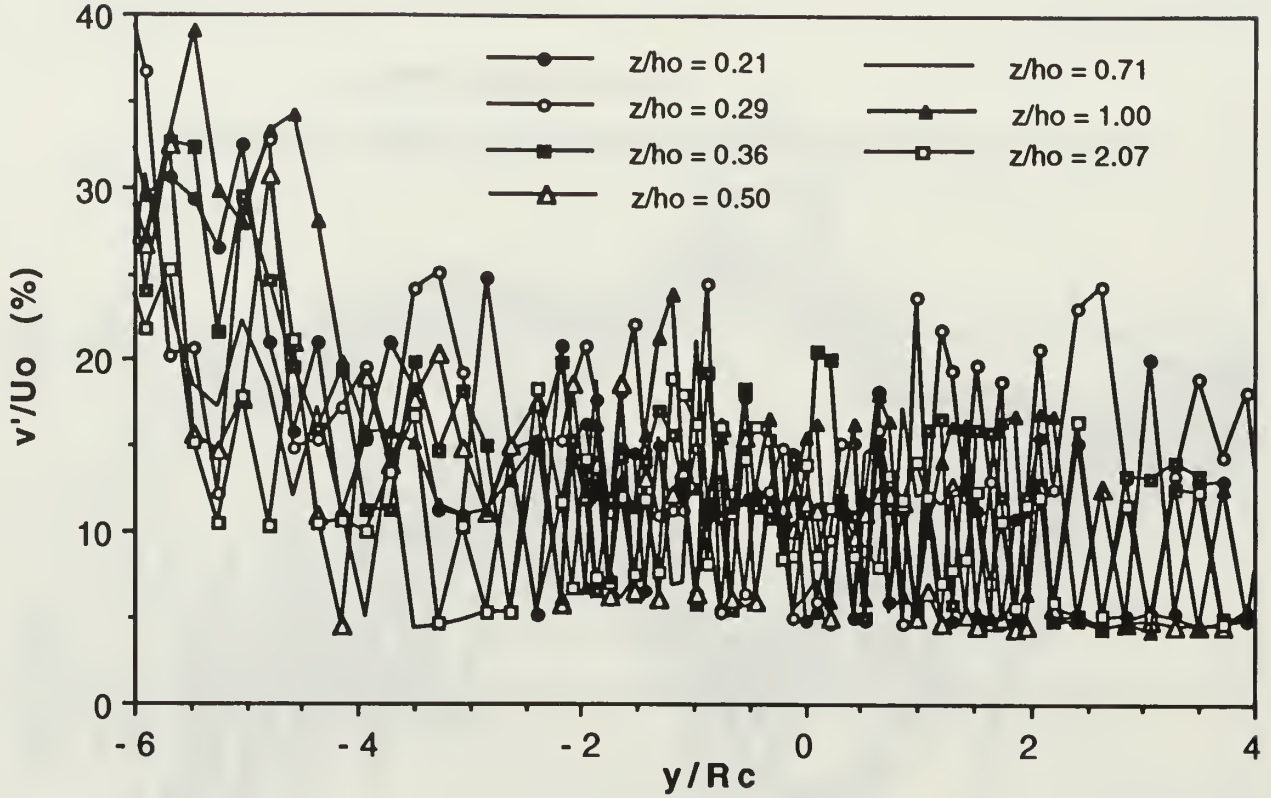

Figure 20. v'/Uo (%) versus y/Rc for vortex depth of ho/Rc = 1.15 below the free surface

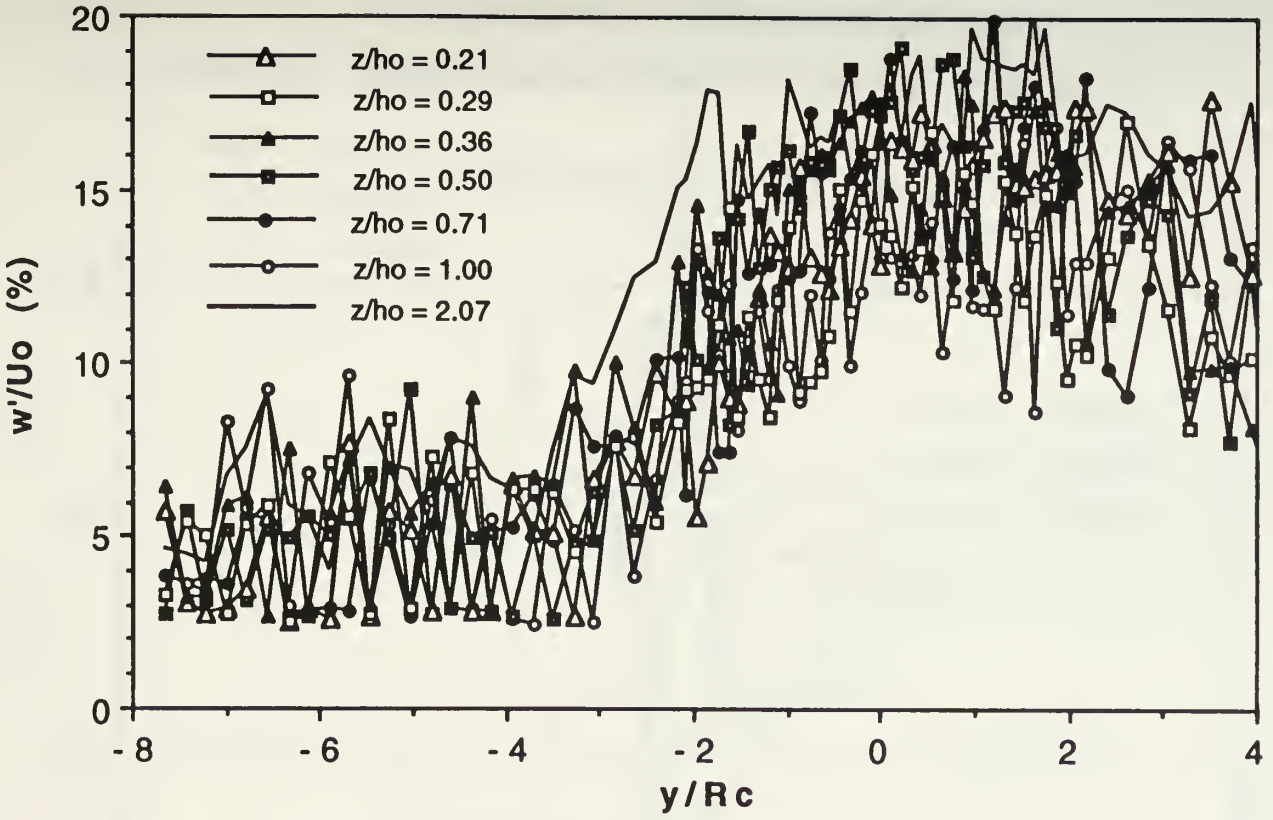

Figure 21. w'/Uo (%) versus y/Rc for vortex depth of ho/Rc = 1.15 below the free surface

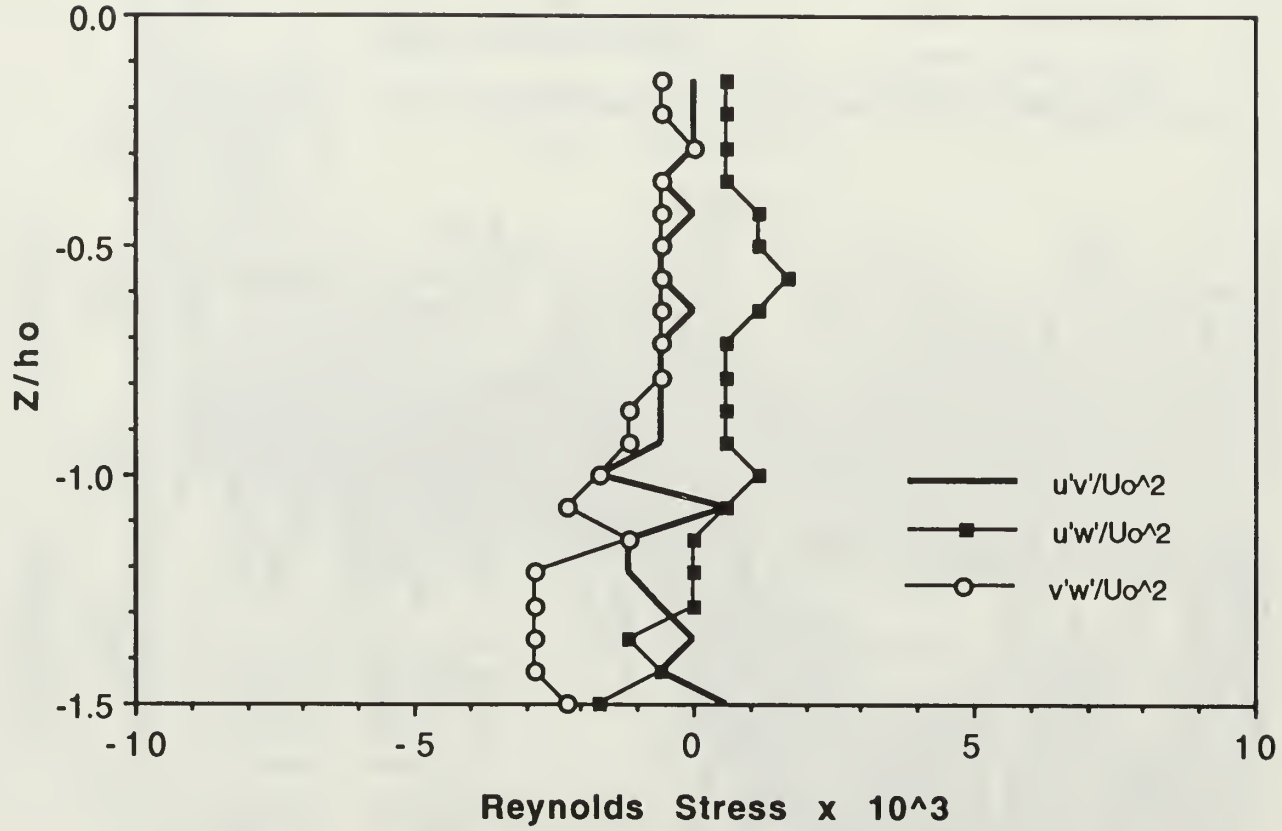

Figure 22. Reynolds Stresses versus z/ho above the vortex centered at a depth of ho/Rc = 1.15 below the free surface

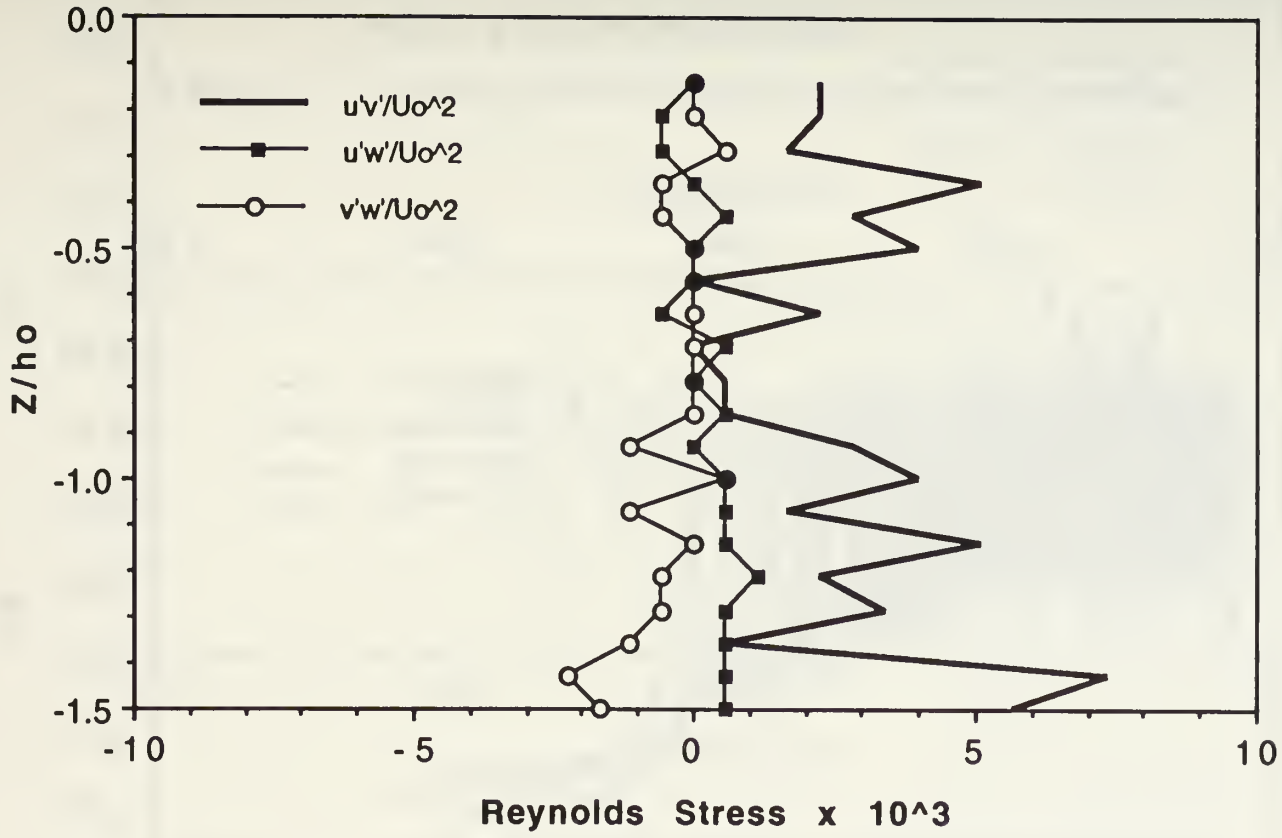

Figure 23. Reynolds Stresses versus z/ho at y/Rc = –1.48 from the vortex centered at a depth of ho/Rc = 1.15 below the free surface

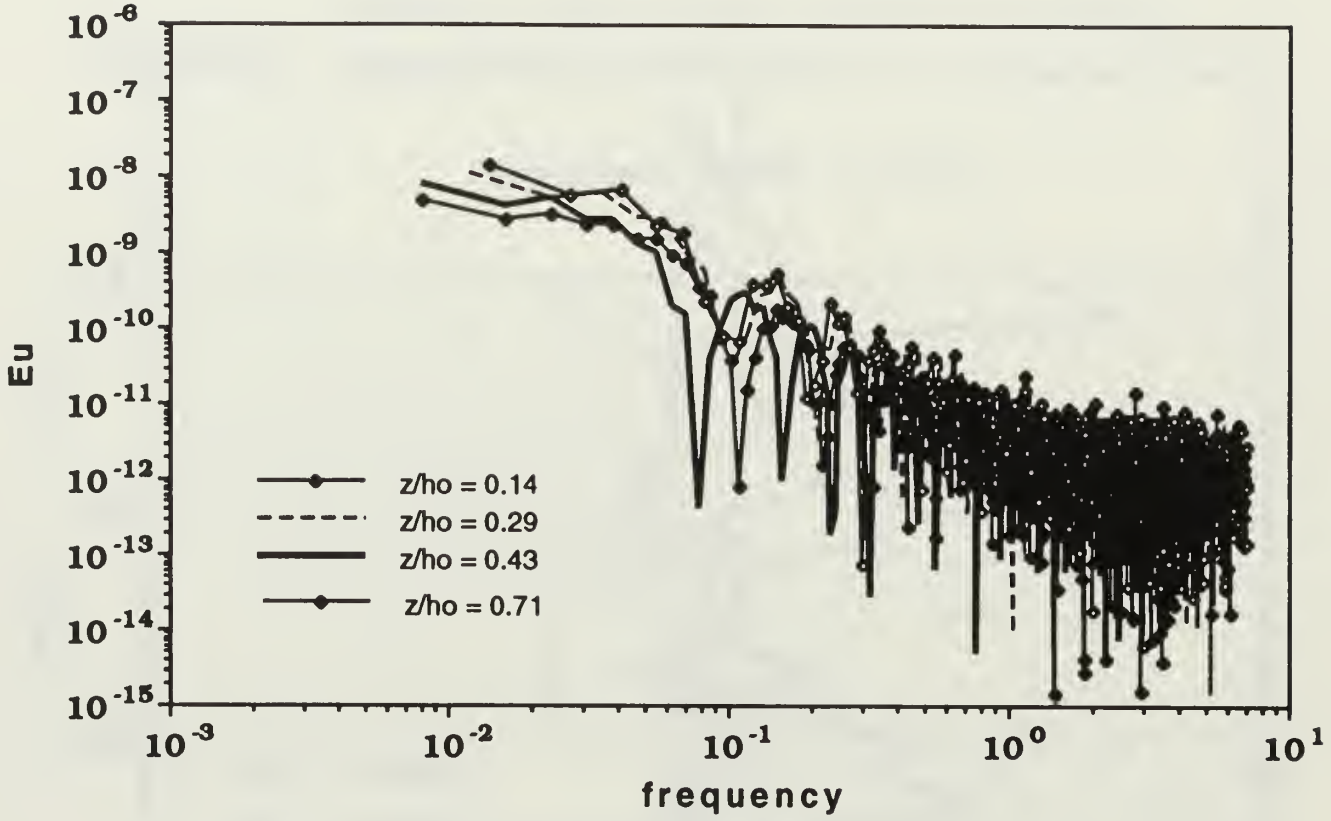

Figure 24. Eu versus Frequency above the vortex centered at a depth of ho/Rc = 1.15 below the free surface

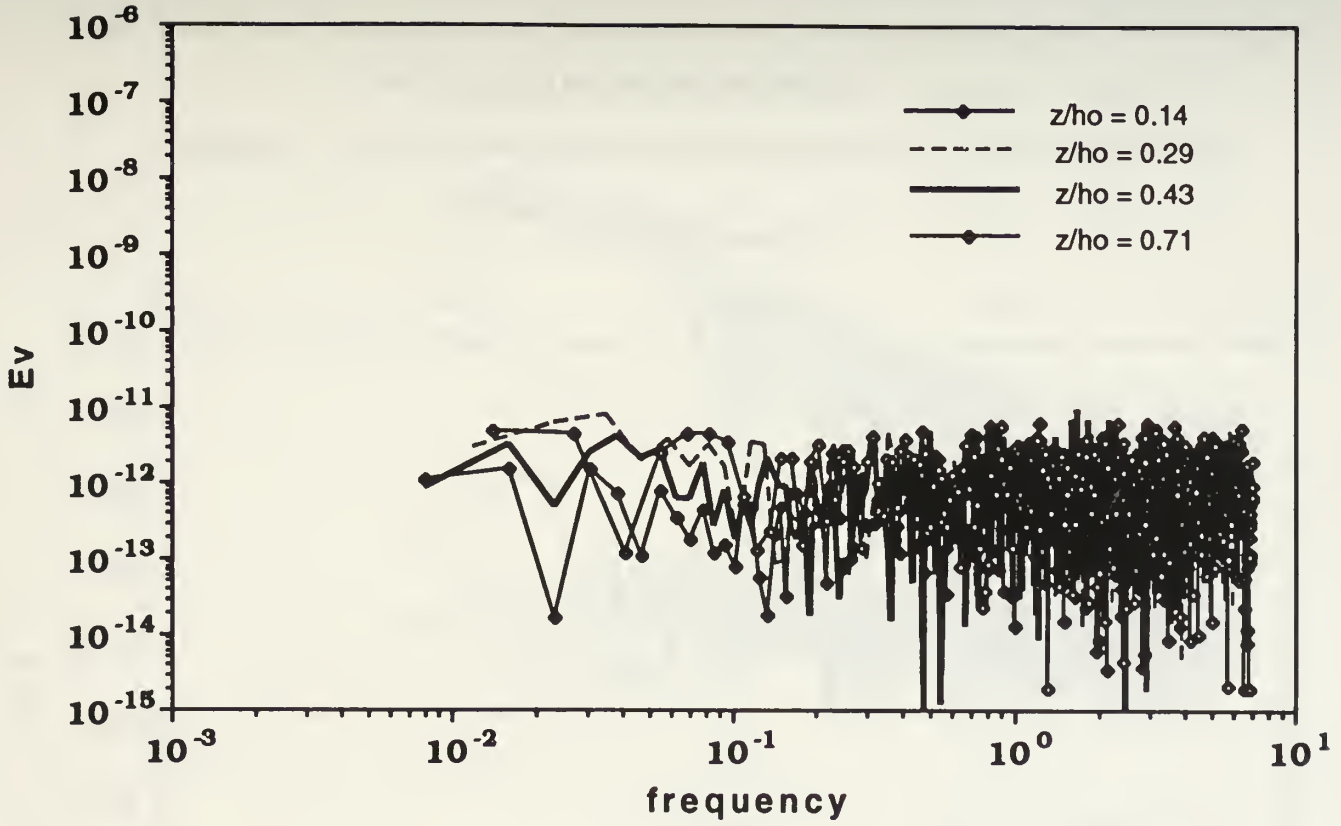

Figure 25. Ev versus Frequency above the vortex centered at a depth of ho/Rc = 1.15 below the free surface

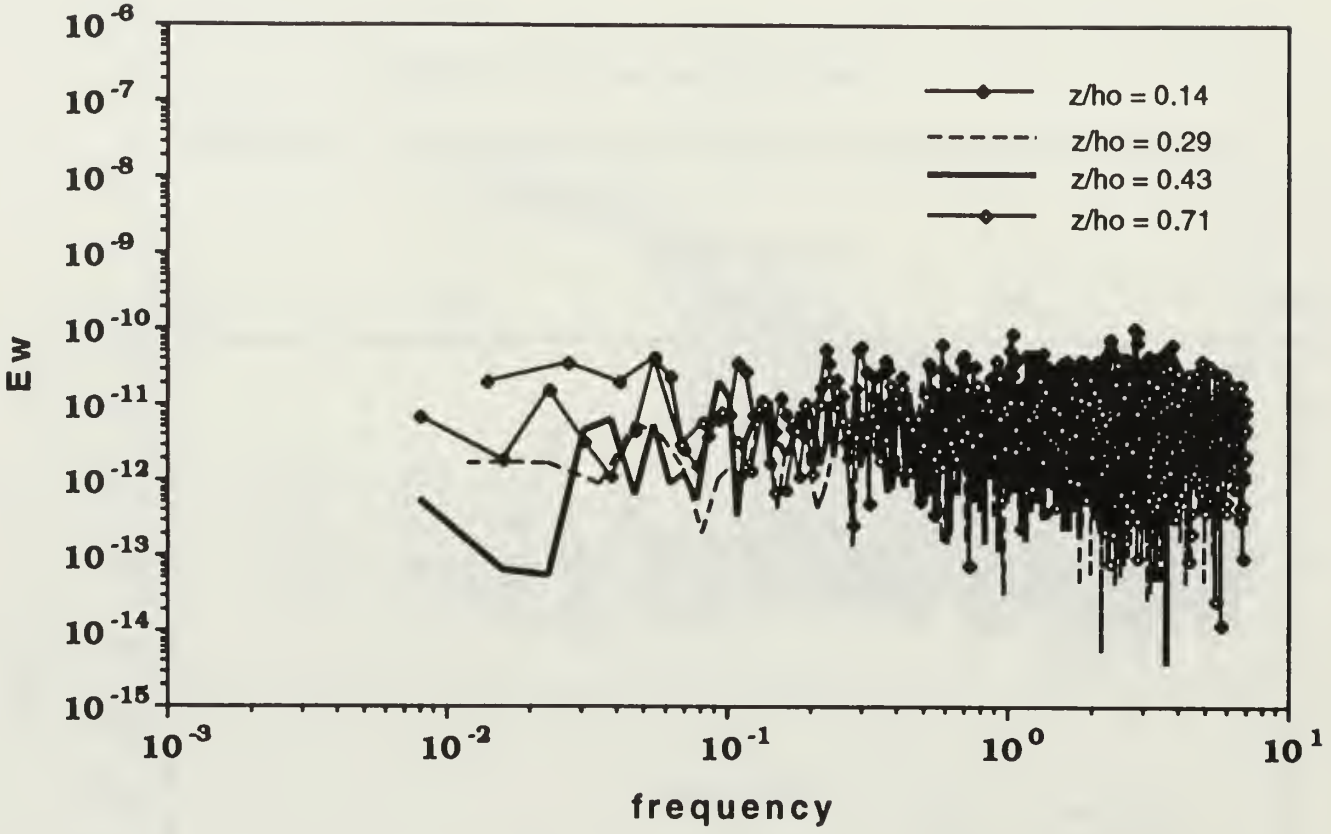

Figure 26. Ew versus Frequency above the vortex centered at a depth of ho/Rc = 1.15 below the free surface

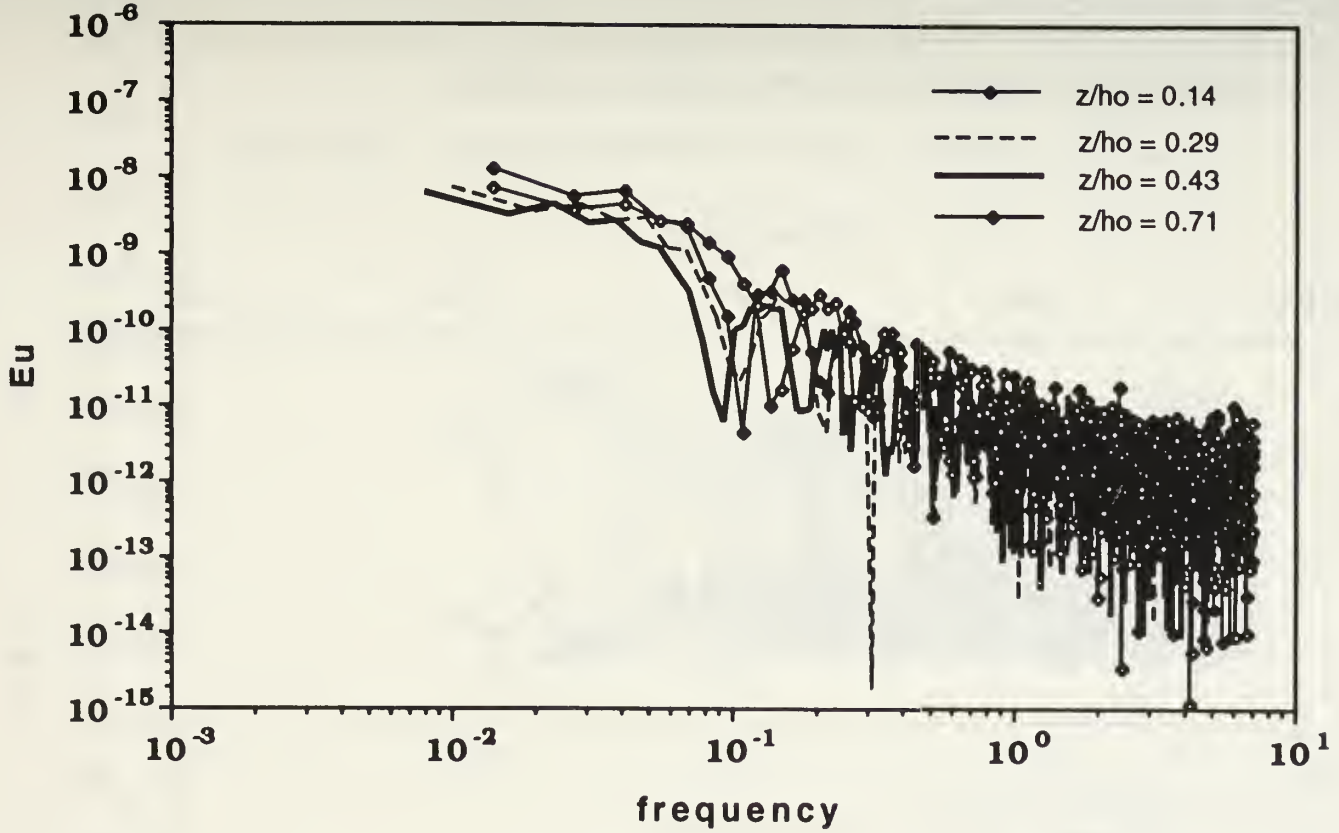

Figure 27. Eu versus Frequency at y/Rc = –1.48 from the vortex centered at a depth of ho/Rc = 1.15 below the free surface

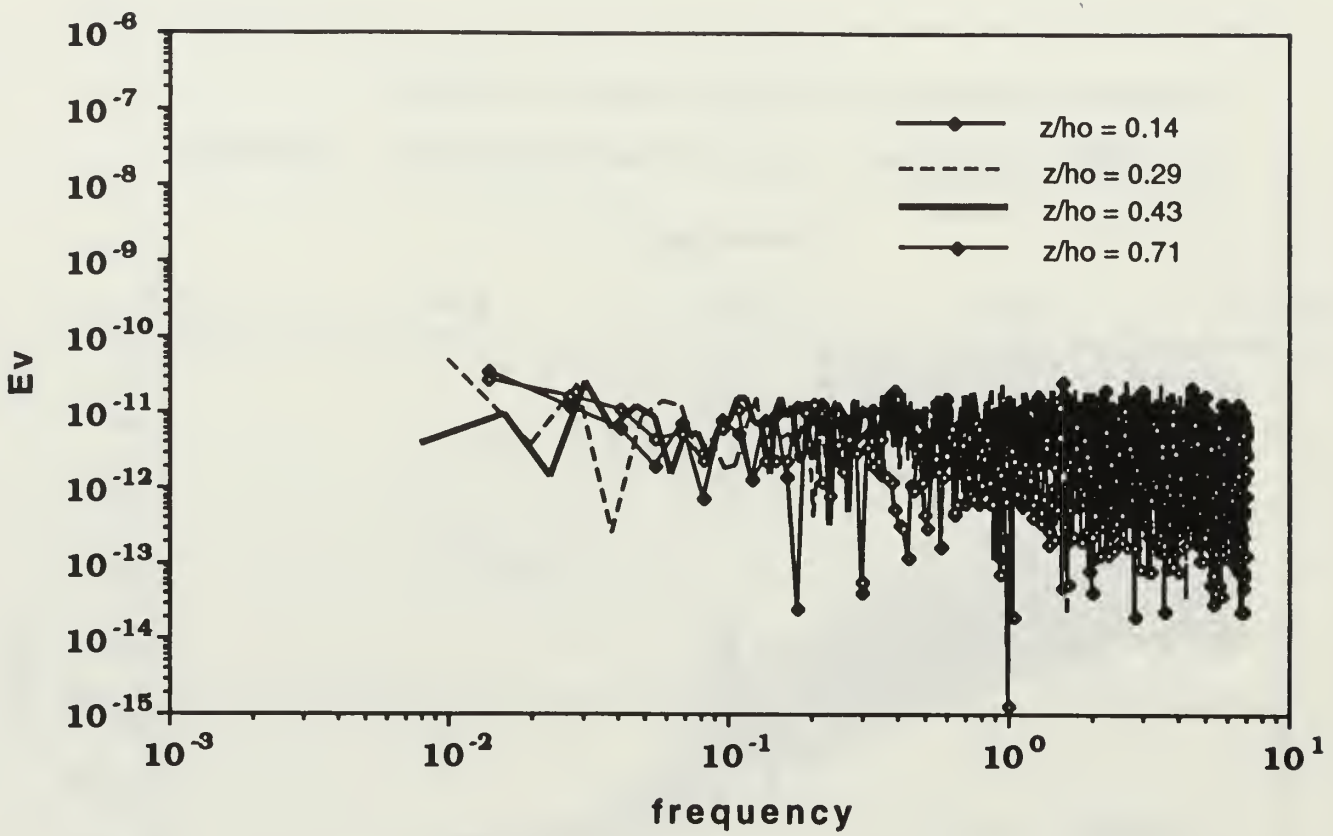

Figure 28. Ev versus Frequency at y/Rc = –1.48 from the vortex centered at a depth of ho/Rc = 1.15 below the free surface

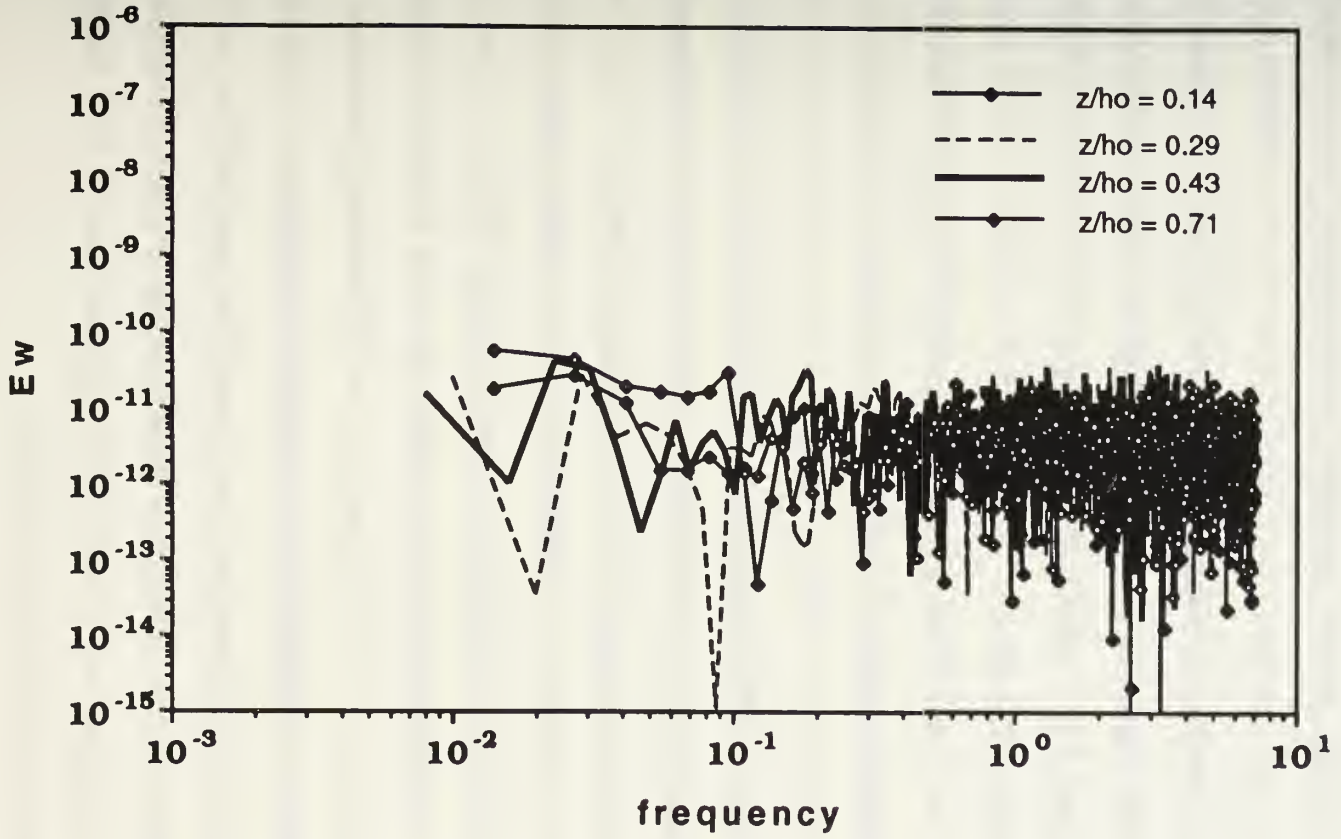

Figure 29. Ew versus Frequency at y/Rc = –1.48 from the vortex centered at a depth of ho/Rc = 1.15 below the free surface

REFERENCES

Anthony, D. G., and Willmarth, W. W., 1992, "Turbulence Measurements in a Round Jet beneath a Free Surface," *Journal of Fluid Mechanics*, Vol. 243, pp. 699-720.

Brandt, A., Geernaert, G., Weinstein, A. I., and Dugan, J. P., 1992, "Sub-Mesoscale Air-Sea Interactions–24th International Liege Colloquium on Ocean Hydrodynamics," *Report of the Office of Naval Research European Office*, ESNIB 92-08, pp. 534-537.

Biringen, S., and Reynolds, W., 1981, "Large-Eddy Simulation of the Shear-Free Turbulent Boundary Layer," *Journal of Fluid Mechanics*, Vol. 103, pp. 53-63.

Brumley, B., 1984, "Turbulence Measurements near the Free Surface in Stirred Grid Experiments," *Gas Transfer at Water Surfaces*, W. Brutsaert and H. Jirka, eds., Reidel–Dordrecht, The Netherlands, pp. 83-86.

Brumley, B., and Jirka, H., 1987, "Near-Surface Turbulence in a Grid Stirred Tank," *Journal of Fluid Mechanics*, Vol. 183, pp. 235-263.

Dickey, T. D., Hartman, B., Hammond, D., and Hurst, E., 1984, "A Laboratory Technique for Investigating the Relationship between Gas Transfer and Fluid Turbulence," *Gas Transfer at Water Surfaces*, W. Brutsaert and H. Jirka, eds., Reidel–Dordrecht, The Netherlands, pp. 93-100.

Dommermuth, D. G., 1992, "The Formation of U-Shaped Vortices on Vortex Tubes Impinging on a Wall with Applications to Free Surfaces," *Physics of Fluids* A, Vol. 4, No. 4, pp. 757-769.

Dommermuth, D. G., 1993, "The Laminar Interactions of a Pair of Vortex Tubes with a Free Surface," *Journal of Fluid Mechanics*, Vol. 246, pp. 91-115.

Hannoun, I. A., Fernando, H. J. S., and List, E. J., 1978, "Turbulence Structure Near a Sharp Density Interface," *Journal of Fluid Mechanics*, Vol. 189, pp. 189-209.

Hannoun, I. A. and List, E. J., 1978, "Turbulent Mixing at a Shear-Free Density Interface," *Journal of Fluid Mechanics*, Vol. 189, pp. 211-234.

Harvey, J. K., and Perry, F. J., 1971, "Flow Field Produced by Trailing Vortices in the Vicinity of the Ground," *American Institute of Aeronautics and Astronautics Journal*, Vol. 9, No. 12, pp. 1659-1660.

Hunt, J. C. R., and Graham, J. M. R., 1978, "Free-Stream Turbulence Near Plane Boundaries," *Journal of Fluid Mechanics*, Vol. 84, pp. 209-235.

Jacquin, L., Leuchter, O., and Geffroy, P., 1989, "Experimental Study of Homogeneous Turbulence in the Presence of Rotation," *Turbulent Shear Flows* 6, J. C. André *et al.*, eds., pp. 46-57, Springer-Verlag.

Komori, S., Nagaosa, R., Murakami, Y., Chiba, S., Ishii, K., and Kuwahara, K., 1993, "Direct Numerical Simulation of Three-Dimensional Open-Channel Flow with Zero-Shear Gas-Liquid Interface," *Physics of Fluids A*, Vol. 5, No. 1, pp. 115-125.

Komori, S., Ueda, H., Ogino, F., and Mizushina, T., 1982, "Turbulence Structure and Transport Mechanism at the Free Surface in an Open Channel Flow," *International Journal of Heat and Mass Transfer*, Vol. 25, No. 4, pp. 513-521.

Kothe, D. B., Mjolsness, R. C., 1992, "RIPPLE: A New Model for Incompressible Flows with Free Surface," *American Institute of Aeronautics and Astronautics Journal*, Vol. 30, No. 11, pp. 2694-2700.

Kothe, D. B., Mjolsness, R. C., and Torrey, M. D., 1991, "RIPPLE: A Computer Program for Incompressible Flows with Free Surfaces," Los Alamos National Lab., LA-12007-MS, Los Alamos, NM.

Lam, K. and Banerjee, S., 1992, "On the Condition of Streak Formation in a Bounded Turbulent Flow," *Physics of Fluids A*, Vol. 4, No. 2, pp. 306-320.

Loewen, S., Ahlborn, B., and Filuk, A. B., 1986, "Statistics of Surface Flow Structures on Decaying Grid Turbulence," *Physics of Fluids*, Vol. 29, No. 8, pp. 2388-2397.

Ohring, S. and Lugt, H. J., 1991, "Interaction of a Viscous Vortex Pair with a Free Surface," *Journal of Fluid Mechanics*, Vol. 227, pp. 47-70.

Rashidi, M., and Banerjee, S., 1988, "Turbulence Structure in Free Surface Channel Flows," *Physics of Fluids*, Vol. 31, No. 9, pp. 2491-2503.

Robinson, S. K., 1991, "Coherent motions in the turbulent boundary layer," *Annual Review of Fluid Mechanics*, Vol. 23, pp. 601-639. (See also, NASA Tech. Mem. 103859, 1991).

Rosenhead, L., 1930, "The Spread of Vorticity in the Wake Behind a Cylinder," *Proceedings of the Royal Society*, Ser. A., Vol. 127, pp. 590-612.

Rouse, H. and Dodu, J., 1955, "Turbulent Diffusion Across a Density Discontinuity," *La Houille Blanche*, Vol. 4, pp. 522-531.

Salvesen, N. and Kerczek, C. von, 1976, "Comparison of Numerical and Perturbation Solutions of Two-Dimensional Nonlinear Water-Wave Problems," *Journal of Ship Research*, Vol. 20, pp. 160-170.

Sarpkaya, T., 1986, "Trailing-Vortex Wakes on the Free Surface," Proceedings of the *16th Symposium on Naval Hydrodynamics*, National Academy Press, Washington, D. C., pp. 38–50.

Sarpkaya, T., 1989, "Computational Methods with Vortices—1988 Freeman Scholar Lecture," *Journal of Fluids Engineering, Transactions of ASME*, Vol. 111, No. 1, pp. 5–52.

Sarpkaya, T., 1992a, "Three-Dimensional Interactions of Vortices with a Free Surface," *American Institute of Aeronautics and Astronautics* Paper No. 92-0059.

Sarpkaya, T., 1992b, "Interaction of a Turbulent Vortex with a Free Surface," *Proceedings of the Nineteenth Symposium on Naval Hydrodynamics*, National Academy Press, Washington, D. C., (in press).

Sarpkaya, T., Elnitsky, J., and Leeker, R. E., 1988, "Wake of a Vortex Pair on the Free Surface," *Proceedings of the 17th Symposium on Naval Hydrodynamics*, National Academy Press, Washington, D. C., pp. 47–54.

Sarpkaya, T. and Neubert, D., 1993, "Interaction of a Streamwise Vortex with a Free Surface," *American Institute of Aeronautics and Astronautics Journal*, Vol. 32, pp. 594-600.

Sarpkaya, T., and Suthon, P. B. R., 1991, "Interaction of a vortex couple with a free surface," *Experiments in Fluids*, Vol. 11, pp. 205-217.

Shabaka, I. M. M., Mehta, R. D., and Bradshaw, P., 1985, "Longitudinal Vortices Imbedded in Turbulent Boundary Layers. Part 1. Single Vortex," *Journal of Fluid Mechanics*, Vol. 155, pp. 37-57.

Smith, C. R., Walker, J. D. A., Haidari, A. H., & Sobrun, U., 1991, "On the dynamics of near-wall turbulence," *Philosophical Transactions of the Royal Society of London*, Vol. A-336, pp. 131-175.

Thomas, N. H. and Hancock, P. E. 1977, "Grid Turbulence Near a Moving Wall," *Journal of Fluid Mechanics*, Vol. 82, pp. 481-496.

Uzkan, T. and Reynolds, W. C., 1967, "A Shear-Free Turbulent Boundary Layer," *Journal of Fluid Mechanics*, Vol. 28, pp. 803-821.

INITIAL DISTRIBUTION LIST

		No. Copies
1.	Defense Technical Information Center Cameron Station Alexandria, VA 22304-6145	2
2.	Librarian, Code 52 Naval Postgraduate School 411 Dyer Rd., Rm. 104 Monterey, CA 93943-5101	2
3.	Department Chairman Mechanical Engineering Department, Code ME Naval Postgraduate School 699 Dyer Rd, Rm. M3 Monterey, CA 93943-5108	1
4.	Professor T. Sarpkaya Mechanical Engineering Department, Code ME-SL Naval Postgraduate School 699 Dyer Rd, Rm. M2 Monterey, CA 93943-5108	5
5.	Naval Engineering Curricular Office Code 34 Naval Postgraduate School 699 Dyer Rd, Rm. 220 Monterey, CA 93943-5109	1
6.	LT Glenn D. Hofert, USN 11719 Sanderson Road Medina, NY 14103	2